4.13 Volcano Seismology

H. Kawakatsu, University of Tokyo, Tokyo, Japan

M. Yamamoto, Tohoku University, Sendai, Japan

4.13.1 Introduction

Volcano seismology is a field of volcanology in which seismological techniques are employed to help understanding the physical conditions and dynamic states of volcanic edifices and volcanic fluid systems to such a level that it eventually contributes to predictions of initiation and cessation of hazardous volcanic activities. Seismology has been a powerful tool for this purpose, especially in the past 10–15 years as new observational and analysis techniques in seismology have become available (e.g., Chouet, 1996a, 1996b; McNutt, 2005); they include digital and broadband seismometry, and array and moment tensor waveform analyses. While the subjects that should be covered under the title of volcano seismology are quite broad and diverse, this chapter, however, neither intends to nor is capable to cover all of its areas; instead we try to focus on some of seismological phenomena which appear to be specific to volcanoes. In a sense, volcano seismology here is a field of seismology which deals with problems specific to volcanic areas. Some of the subjects, such as seismic structure of volcanoes (tomography) and eruption monitoring (seismicity), are therefore intentionally omitted. The readers who are interested in these subjects are advised to refer to the excellent reviews by Chouet (1996a, 1996b, 2003) and McNutt (1996, 2002, 2005).

4.13.2 Volcanic Seismic Signals

For seismologists who have only observed seismograms of ordinary faulting earthquakes, the most intriguing aspect of volcano seismology may be the ample variety of waveforms recorded in volcanic environments. Such volcanic seismic signals range from totally chaotic continuous vibrations lasting for minutes, hours, or sometimes days to purely monotonic vibrations decaying with constant damping rates; they often show several spectral peaks whose frequency may vary during the course of volcanic activities, possibly reflecting the change of physical conditions of volcanic fluid systems; when eruptions occur, variety of long-period signals up to as long as a few hundred seconds are generated and sometimes observed at seismic stations around the world. In the following, some of such intriguing volcanic seismic signals will be presented.

Terminology. Based on their appearance on short-period seismometers, volcanic seismic signals have been traditionally classified into four types: high-frequency or A type, low-frequency or B type, explosion quakes, and volcanic tremors (e.g., Minakami, 1974; for the detail of different terminology, see table 1 of McNutt (1996)). In this chapter, following this tradition, we use high frequency for frequencies higher than 5 Hz, and low frequency for frequencies between 5 and 0.5 Hz. On the other hand, the usage of period remains a complicated issue in volcano seismology; the most widely accepted notation to describe volcanic seismic signals is that of Chouet (1996b), in which events of about 1 s are called 'long-period' (LP) events and those with longer periods are called 'very-long-period' (VLP) and 'ultra-long-period' (ULP) events. This definition, however, contradicts with the conventional usage of period in traditional earthquake seismology, where periods longer than the dominant period of the ambient microseismic noise (around 5–10 s) are called 'long-period' (Aki and Lee, 2003; McNutt, 1996, 2005). In this chapter, as we try to cover the subject in a wider context of seismology, we follow the convention of earthquake seismology, and use the term long-period for periods longer than 5 s and short period for periods shorter than or around 1 s; for events with a period longer than 50 s, we may also use very long-period. To avoid confusion, whenever appropriate, we will try to associate actual number in seconds to describe a period, for example long-period (10 s).

4.13.2.1 Signals Observed by Short-Period Seismometers

The conventional seismometry at active volcanoes, except for a few rare cases, has been conducted using short-period seismometers. Even with such band-restricted sensors, wide varieties of waveforms recorded in volcanoes have led scientists to wonder what may be the origins of those signals. **Figure 1** shows a classical yet the most fascinating one of those

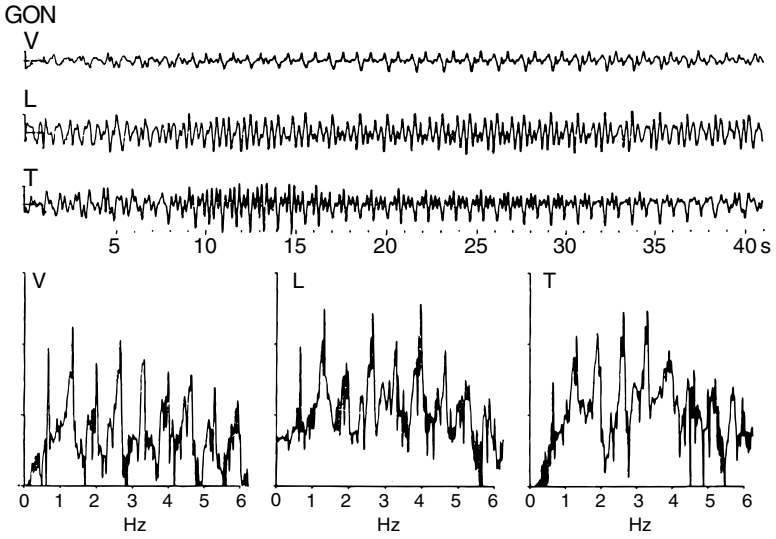

Figure 1 Volcanic tremor observed at Sakurajima. Top three traces show 40 s long seismograms for vertical, longitudinal, and transverse components. Corresponding spectra are shown below. Adapted from Kamo K, Furuzawa T, and Akamatsu J (1977) Some natures of Volcanic micro-tremors at the Sakurajima Volcano. *Bulletin of the Volcanological Society of Japan* 22: 41–58.

recordings of volcanic tremors observed at Sakurajima Volcano, Japan (Kamo *et al.*, 1977). Volcanic tremors are those sustained ground vibrations commonly observed at volcanoes, typically lasting for longer than 1 min, up to hours or days; they often show periodic spectral features as seen here with the lowest peak frequency around 1 Hz. During the course of activities, relative spectral content and peak frequencies may vary from time to time.

Figure 2 shows examples from Redoubt Volcano, Alaska, where different types of events are displayed: from the top, (A) high-frequency or volcano-tectonic (VT) earthquake, which most likely represents an ordinary brittle failure on a fault, (B) hybrid or mixed-frequency event, (C) low-frequency (LF) event with frequency around 1 Hz, and (D) volcanic tremor. Note that the volcanic tremor here appears more random compared to those in **Figure 1**, and also its frequency content seems similar to that of the low-frequency event (C). It is sometimes considered that tremors and low-frequency events share a common excitation mechanism.

Low-frequency events in some volcanoes show characteristic similar spindle-shape waveforms, suggesting a possible common origin for these events in different volcanoes.

Explosion quakes are observed when explosive eruptions occur, and often associated with a high-frequency arrival on seismograms due to a shock wave originated at the vents. **Figure 3** shows series of such events recorded in Langila Volcano, Papua New Guinea (Mori *et al.*, 1989), sorted by the ratio of ground-transmitted explosion-wave and air-wave amplitudes. As those without an air wave are classified as low-frequency events, this figure also indicates that explosion quakes and low-frequency events may share a common origin.

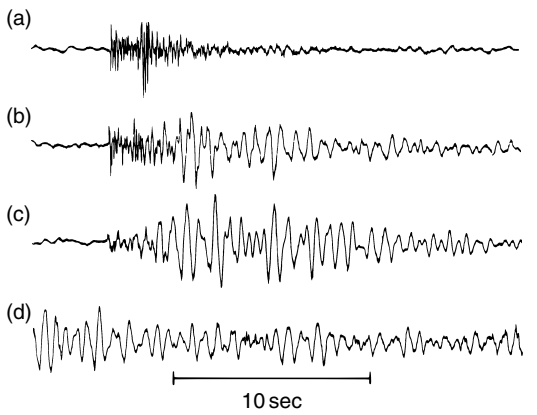

Figure 2 Typical waveforms observed at Redoubt. After McNutt SR (1996) Seismic monitoring and eruption forecasting of volcanoes: A review of the state-of-the-art and case histories. In: *Monitoring and Mitigation of Volcano Hazards*, pp. 99–146. New York: Springer.

As noted earlier, the spectral content of these low-frequency volcanic seismic signals may vary throughout the course of activities. **Figure 4** shows such an example from Montserrat Volcano, West Indies; the temporal change of the system prior to an explosion is clearly manifested.

It appears clear that the low-frequency nature of these seismograms is the most characteristic of volcanic seismic signals. Although they are characterized here just in terms of the frequency content, there exist similarities and diversities among them; their origins may be different from a volcano to another, and may change from time to time even in a single volcano. Understanding of their origins and monitoring of their appearances to infer physical conditions and dynamic states of volcanic edifices and volcanic fluid systems are interesting and challenging tasks.

Deep (volcanic) low-frequency signals. Most of volcanic seismic signals originate within a shallow part of the crust (<5 km). There are, however, a certain type of volcanic seismic signals which originate either from the lower crust or from the uppermost mantle (15–50 km) right beneath active volcanoes. As they show similar low-frequency content as volcanic tremors, they are often called deep low-frequency volcanic tremors (or events). They are now reported in many volcanoes around the world (e.g., Aki and Koyanagi, 1981; Pitt and Hill, 1994; Hasegawa and Yamamoto, 1994; White, 1996; Nakamichi *et al.*, 2003). As deep low-frequency volcanic tremors may be related with deep magma-supplying system of volcanoes, understanding of their origin seems extremely important for the long-term prediction of the activities of volcanoes.

4.13.2.2 Broadband Signals

Availability of broadband seismic records has brought wider perspectives in our view of volcanic activities. **Figure 5** shows a very good example observed at Satsuma-Iwojima Volcano, Japan (Ohminato and Ereditato, 1997). The short-period sensor recording at ST3 shows amplitude modulation

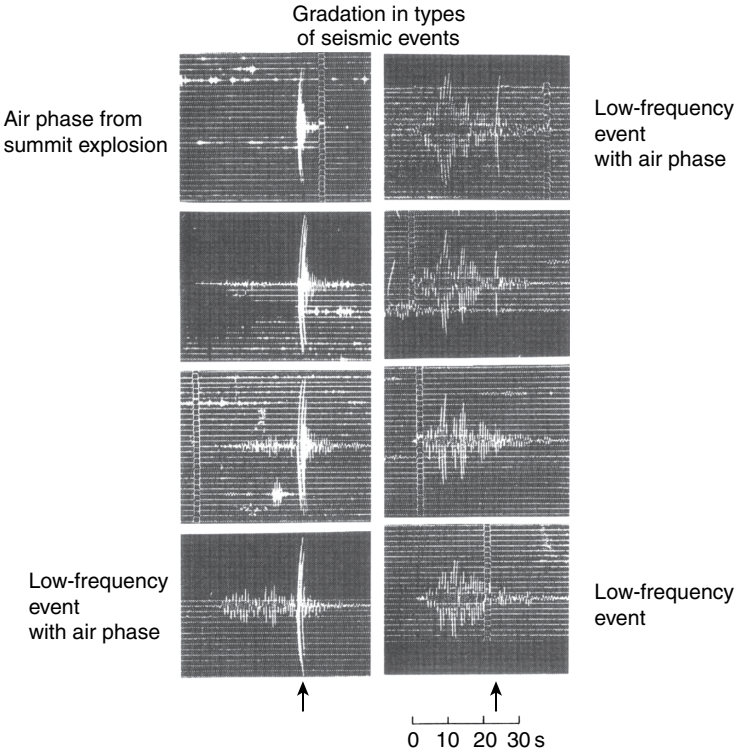

Figure 3 Range of volcanic seismic signals from the high-frequency air-wave phase to LF event observed at Langila. Arrows indicate timings of air-wave phases. Adapted from Mori J, Patia H, and McKee C, *et al*. (1989) Seismicity associated with eruptive activity at Langila Volcano, Papua New Guinea. *Journal of Volcanology Geothermal Research* 38: 243–255.

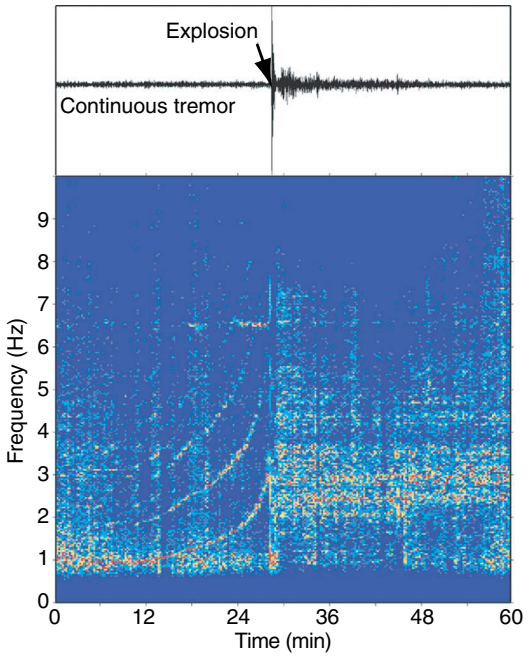

Figure 4 Example of tremor at Montserrat before an explosion. After Jousset P, Neuberg J, and Sturton S (2003) Modelling the time-dependent frequency content of low-frequency volcanic earthquakes. *Journal of Volcanology Geothermal Research* 128: 201–223.

of high-frequency signal with a periodicity of 46–50 min. When this amplitude becomes small, the lowpass-filtered broadband record at ST1 shows long-period (10 s) spike-like signals. This synchronicity of two different band signals continues, while the exact periodicity may fluctuate. Such an interplay of different band signals forces us to view the origin of these signals as a system (i.e., volcanic fluid system).

Figure 6 is another such example of a broadband record of a small phreatic eruption observed at Aso Volcano, Japan (Kaneshima *et al*., 1996; Kawakatsu *et al*., 2000). While the integrated displacement record exhibits a very long-period (>100 s) signal corresponding to the inflation and deflation stages of a crack-like conduit (Yamamoto *et al*., 1999) before and during the eruption, the raw velocity record exhibits short-period signals apparently due to the quick flow of volcanic fluids only seen in the deflation stage (i.e., eruption). Again signals seen in two different bands allow us to vividly image the process of the eruption of a volcanic fluid system. Different physics apply at different frequencies, and this makes volcanic seismic signals essentially broadband.

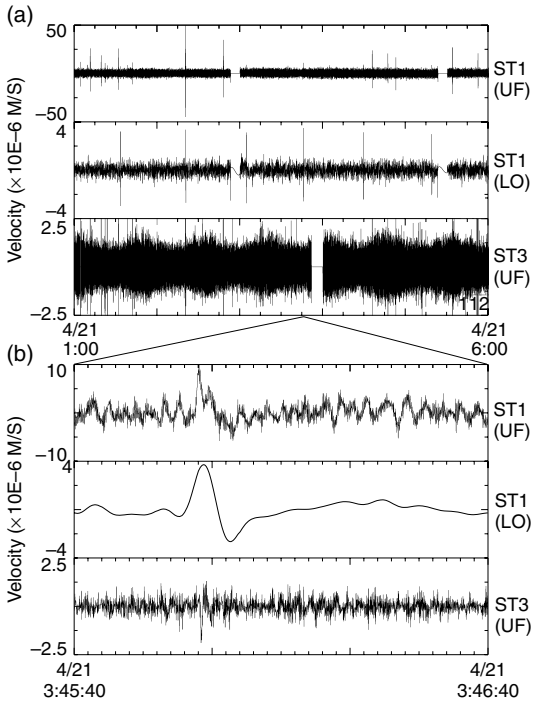

Figure 5 (a) Five-hour records of vertical components of velocity at Satsuma-Iwojima. A trace lowpass-filtered (LO) at 0.2 Hz is shown in between the two unfiltered records. (b) Expansion of the 1 min portion of the top panel. Adapted from Ohminato T and Ereditato D (1997) Broadband seismic observations at Satsuma-Iwojima Volcano, Japan. *Geophysical Research Letters* 24: 2845–2848.

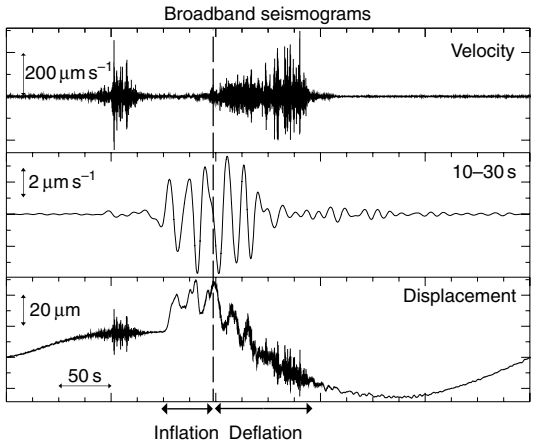

Figure 6 Broadband waveforms of a phreatic eruption observed at Aso. Adapted from Kawakatsu H, Kaneshima S, and Matsubayashi H, *et al*. (2000) Aso94: Aso seismic observation with broadband instruments. *Journal of Volcanology Geothermal Research* 101: 129–154.

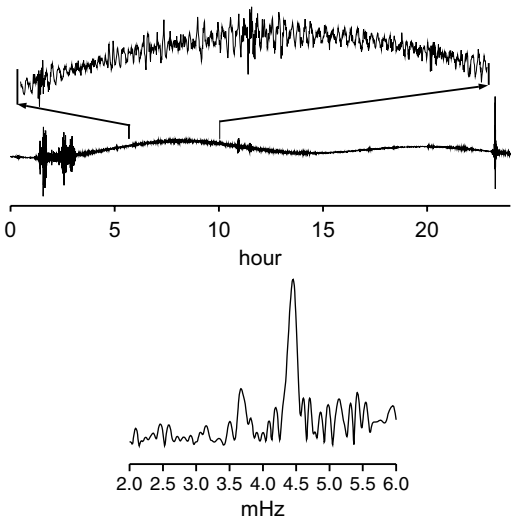

Figure 7 Broadband record of the Pinatubo eruption in 1991 observed in Japan. Adapted from Watada S (1995) *Part I: Near-source Acoustic Coupling Between the Atmosphere and the Soild Earth During Volcanic Eruptions*. PhD Thesis, California Institute of Technology.

Global observation. The last example (**Figure 7**) comes from the recordings of very long-period (200–400 s) seismic signals generated by the eruption of Pinatubo Volcano, Philippines, observed at broadband stations around the world (Kanamori and Mori, 1992; Widmer and Zürn, 1992). The long-period disturbances of the atmosphere generated by the eruption clouds are transmitted back to the solid Earth through the coupling between the two systems. Two spectral peaks observed in the seismic records are well explained by a theory which treats the solid Earth and the atmosphere as a single system (Watada, 1995); such a coupling between the solid and fluid parts of the Earth is also observed in so-called background free oscillations of the Earth (Nishida *et al.*, 2000). The broadband recordings of the Pinatubo eruption appear to have accelerated the emergence of a new class of seismology which treats the solid Earth, atmosphere, and ocean as a single system (cf. Chapter 4.14).

4.13.3 Description of Volcanic Seismic Sources

The diversity of observed volcanic seismic signals partly reflects the wide variety of seismic source geometries and dynamics present in active

volcanoes. A general kinematical description of seismic sources in terms of 'moment tensor' and 'single force' has become common in volcano seismology, and the waveform inversion solving for them has been becoming a general tool to understand the generation mechanisms of long-period signals obtained with broadband instruments.

4.13.3.1 Equivalent Forces of General Seismic Sources

The concept of the seismic moment tensor was first introduced by Gilbert (1970) as a description of seismic sources more general than the conventional double-couple description. Later Backus and Mulcahy (1976) gave a physical basis for such a general description within the framework of linear elastodynamics by introducing concepts of indigenous source and stress glut. An indigenous source is a seismic source which originates within the Earth, and its equivalent force system exerts neither total force nor total torque at any instance to the Earth. Seismologists, however, soon realized that there exist such indigenous seismic events which require single force equivalent force systems (e.g., Kanamori and Given, 1982; Kanamori *et al.*, 1984; Hasegawa and Kanamori, 1987; Kawakatsu, 1989); most of them happened to occur around active volcanoes. To circumvent this apparent conflict, Takei and Kumazawa (1994) extended Backus and Mulcahy's treatment to include fluid-dynamical description with a mass advection term, and introduced a concept of inertial glut; they further gave a clear definition of single force (and torque) source as a momentum (and angular momentum) exchange between the seismic source volume and the rest of the Earth. In the following, we briefly summarize their treatment.

To make the argument simple, we omit the Earth's self-gravity in the following; although gravity often takes the central role generating single forces in the actual Earth, this simplification does not alter the essence of the argument presented below. The true Eulerian equation of motion of the Earth without external force may be written as

$$\rho^{\mathrm{t}} D_t^2 u_j = \partial_i S_{ij} \qquad [1]$$

where $\rho^{\mathrm{t}}(\mathbf{x}, t)$ denotes the true density, $u_j(\mathbf{x}, t)$ is the displacement, $S_{ij}(\mathbf{x}, t)$ is the true stress field, and D_t is the particle derivative $D_t = \partial_t + v_k \partial_k$ with $v_k(\mathbf{x}, t)$ as the velocity. We compare this true equation of motion with the linear elastodynamic equation of motion,

$$\rho^{\mathrm{m}} \partial_t^2 u_j = \partial_i \phi_{ij} \qquad [2]$$

where $\rho^{\mathrm{m}}(\mathbf{x}, t)$ and $\phi_{ij}(\mathbf{x}, t)$ respectively denote the model density and model stress field due to the linear stress–strain constitution equation (Hooke's law), which we use to describe the wave propagation in the Earth. The equivalent body force $\gamma_j^V(\mathbf{x}, \mathrm{t})$ in the linear elastodynamic system arises as the difference of the two equations [1] and [2],

$$\rho^{\mathrm{m}} \partial_t^2 u_j = \partial_i \phi_{ij} + \gamma_j^V \qquad [3]$$

where

$$\gamma_j^V = \gamma_j^S + \gamma_j^D \qquad [4]$$

with

$$\gamma_j^S = -\partial_i \Gamma_{ij} = -\partial_i (\phi_{ij} - S_{ij}) \qquad [5]$$

$$\gamma_j^D = \rho^{\mathrm{m}} \partial_t^2 u_j - \rho^{\mathrm{t}} D_t^2 u_j \qquad [6]$$

$\Gamma_{ij}(\mathbf{x}, t) = \phi_{ij}(\mathbf{x}, t) - S_{ij}(\mathbf{x}, t)$ in [5] is the stress glut introduced by Backus and Mulcahy (1976) which represents failure of Hooke's law due to some nonlinear effect in the source region, and is zero outside of the source region. The second term in [4], $\gamma_j^D(\mathbf{x}, t)$, is named as inertial glut by Takei and Kumazawa (1994), and is the difference of the inertial forces in the actual value and in the model, which is again zero outside of the source region. It can be shown that total force and total torque due to $\gamma_j^S(\mathbf{x}, t)$ integrated over the volume is zero at any instance, while those due to the inertial glut $\gamma_j^D(\mathbf{x}, t)$ are necessarily not.

The spatial integral of [6] over the whole space

$$\gamma_j^{(0)D} = \int (\rho^{\mathrm{m}} \partial_t^2 u_j - \rho^{\mathrm{t}} D_t^2 u_j) \mathrm{d}V \qquad [7]$$

can be shown to be

$$\gamma_j^{(0)D} = -\partial_t^2 \int_{V_s} (\rho^{\mathrm{t}} - \rho^{\mathrm{m}}) u_j \mathrm{d}V \qquad [8]$$

which shows that $\gamma_j^{(0)D}(t)$ originates from a difference between ρ^{t} and ρ^{m} in the source region V_s and thus may not vanish. On the other hand, it is shown that the time integral of $\gamma_j^{(0)D}(t)$ during the event vanishes, that is,

$$\int_0^\infty \gamma_j^{(0)D} \mathrm{d}t = 0 \qquad [9]$$

the requirement that any indigenous source has to satisfy. The authors further defined single force and torque sources as linear and angular momenta

exchange between the source region and the rest of the Earth, and showed that, in the long-period limit, the single force source is equal to $\gamma_j^{(0)D}(t)$.

4.13.3.2 The Seismic Moment Tensor

The spatial integral of stress glut is the seismic moment tensor M_{ij} which describes the overall feature of the seismic source. When the wavelength of observed seismic waves is much longer than the spatial extent of the source, we may approximate the source by a point source moment tensor. Each component of M_{ij} corresponds to one set of opposing forces (dipole or force couple; **Figure 8**). The seismic moment tensor is a symmetric second-order tensor, and thus has six independent components, while a double-couple equivalent body force for a shear dislocation has only four degrees of freedom. These two extra degrees of freedom in the moment tensor are called non-double-couple components. For the general discussion on non-double-couple components, readers may refer to the following review articles (Julian *et al.*, 1998; Miller *et al.*, 1998). Seismic sources observed in the volcanic environments often show non-double-couple components. The end members of such non-double-couple sources are discussed below.

Spherical source. Let us consider an initial condition that a reservoir contains a certain amount of volcanic fluid (V) under a static pressure P. When a sudden volume increase of ΔV (measured under the same pressure condition) is introduced in the reservoir, either due to an injection of a new volcanic fluid or a thermal expansion, the reservoir should expand and act as a seismic source. This volumetric increase ΔV corresponds to the stress-free volumetric strain introduced by Eshelby (1957) (Aki and Richards, 2002, p. 53) and characterizes the amount of the increase of the volcanic fluid. On the other hand, due to the confining pressure of the surrounding elastic medium (matrix), the actual volumetric increase of the reservoir ΔV_{m} may be smaller than ΔV, the ratio $\Delta V_{\mathrm{m}}/\Delta V$ depending on the geometry of the reservoir, with a resultant pressure increase ΔP_{m}.

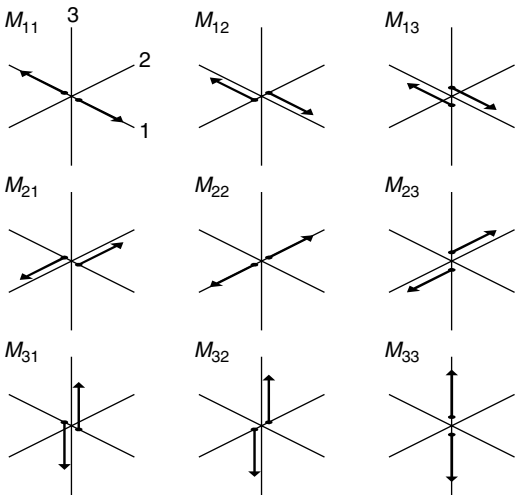

Figure 8 Nine force couples corresponding to moment tensor components.

The corresponding moment tensor for a spherical reservoir is given as

$$M = \Delta V \begin{pmatrix} \lambda + \frac{2}{3}\mu & 0 & 0 \\ 0 & \lambda + \frac{2}{3}\mu & 0 \\ 0 & 0 & \lambda + \frac{2}{3}\mu \end{pmatrix} \quad [10]$$

where the ratio

$$\frac{\Delta V_{\mathrm{m}}}{\Delta V} = \frac{\lambda + (2/3)\mu}{\lambda + 2\mu} \quad [11]$$

and the actual volumetric strain and pressure increase may be related as

$$\Delta P_{\mathrm{m}} = \frac{4}{3}\mu \frac{\Delta V_{\mathrm{m}}}{V} \quad [12]$$

(Aki and Richards, 2002, p. 61). As the actual volumetric change ΔV_{m} is also the volume change often used in geodetic analysis (e.g., Mogi, 1958), we propose to call this 'Mogi volume' to distinguish it from the stress-free volume increase ΔV.

Cylinder. A moment tensor corresponding to the radial expansion of a cylinder whose symmetry axis is x_1 may be given as

$$M = \Delta V \begin{pmatrix} \lambda & 0 & 0 \\ 0 & \lambda + \mu & 0 \\ 0 & 0 & \lambda + \mu \end{pmatrix} \quad [13]$$

where

$$\frac{\Delta V_{\mathrm{m}}}{\Delta V} = \frac{\lambda + \mu}{\lambda + 2\mu} \quad [14]$$

and

$$\Delta P_{\mathrm{m}} = \mu \frac{\Delta V_{\mathrm{m}}}{V} \quad [15]$$

Tensile crack. A moment tensor corresponding to an opening of a thin crack in the direction of x_1-axis may be given as

$$M = \Delta V \begin{pmatrix} \lambda + 2\mu & 0 & 0 \\ 0 & \lambda & 0 \\ 0 & 0 & \lambda \end{pmatrix} \qquad [16]$$

In case of a thin crack, two volumetric changes turn out to be the same. The Mogi volume here is given as $\Delta V = \Delta V_{\mathrm{m}} = S \cdot \Delta \bar{u}$, where S and $\Delta \bar{u}$ are the crack area and opening width, respectively, and it is often referred to as 'potency' in seismological literatures (e.g., Ben-Menahem and Singh, 1981).

Compensated linear vector dipole. The isotropic components of the moment tensors of these three volumetric sources, when expressed in terms of stress-free volumetric change ΔV, are the same:

$$I = \frac{1}{3}\mathrm{trace}(M) = \left(\lambda + \frac{2}{3}\mu\right)\Delta V = \kappa \Delta V \qquad [17]$$

where κ is the bulk modulus of the elastic matrix. When a movement of magma from a reservoir to another excites seismic waves, such a seismic source should be observed as a summation of two volumetric sources with opposite signs. Equation [17] indicates that the corresponding moment tensor has zero isotropic component called compensated linear vector dipole (CLVD) by Knopoff and Randall (1970) (**Figure 9**).

Determination and interpretation of a moment tensor. Due to structural complexities of volcanic edifices, the conventional first motion polarity analysis method to determine source mechanisms of volcanic events is unlikely to give reliable estimates of moment tensors. Although the amplitude of radiated seismic waves contains more information, often the absolute amplitude also suffers from structural complexities. Methods that utilize relative amplitudes of waves which share common ray paths, such as the spectral ratio method of Nishimura *et al.* (1995), the amplitude ratio method of Julian and Foulger (1996), and the relative moment tensor inversion method of Dahm (1996), appear to be better suited; among them, the linear-programming approach of Julian and Foulger (1996) has been extensively used to show the existence of many non-double-couple earthquakes in different volcanic/geothermal environments (e.g., Ross *et al.*, 1996; Foulger *et al.*, 2004).

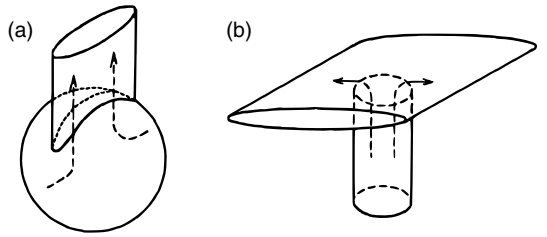

Figure 9 Geometry of selected transport models. Adapted from Chouet B (1996b) New methods and future trends in seismological volcano monitoring. In: *Monitoring and Mitigation of Volcano Hazards*, pp. 23–97 New York: Springer.

An arbitrary moment tensor observed at volcanoes may be decomposed as a linear combination of those four end-member moment tensors (plus a double couple). As such a decomposition is nonunique, there can be different decompositions for a given moment tensor, and thus there exists always nonuniqueness in interpreting moment tensor solutions in terms of actual phenomenon that is occurring at volcanoes. It is often a custom to choose the simplest possible one or to choose one which is most consistent with known source geometry of corresponding volcano (e.g., the presence of known crack-like conduit). Without such *a priori* information, on the other hand, one may wish to display a full moment tensor. The source-type plot introduced by Hudson *et al.* (1989) may be a useful tool to help interpreting different moment tensors observed in different volcanic environments (e.g., Foulger *et al.*, 2004; **Figure 10**). It displays moment tensors without regard to their orientations, and different types of moment tensors (different in relative magnitudes of principal moments) are projected on a rhombic plane in such a way that the area is proportional to the probability of the occurrence of different source types.

4.13.3.3 The Single Force

As described above, the single force equivalent body force is due to a momentum exchange between the source volume and the rest of the Earth. Whenever a part of the Earth is detached from the rest and gains a momentum, the counter force of this acceleration is felt by the rest of the Earth. As the detached mass eventually has to stop somehow, there must be a deceleration stage in this process, giving another counter force with the opposite direction. The total of these two counter forces must cancel out as required from [9].

The single force equivalence of long-period seismic waves excited by a landslide and explosions associated with the 1980 eruption of Mt. St. Helens was established by Kanamori and Given (1982) and

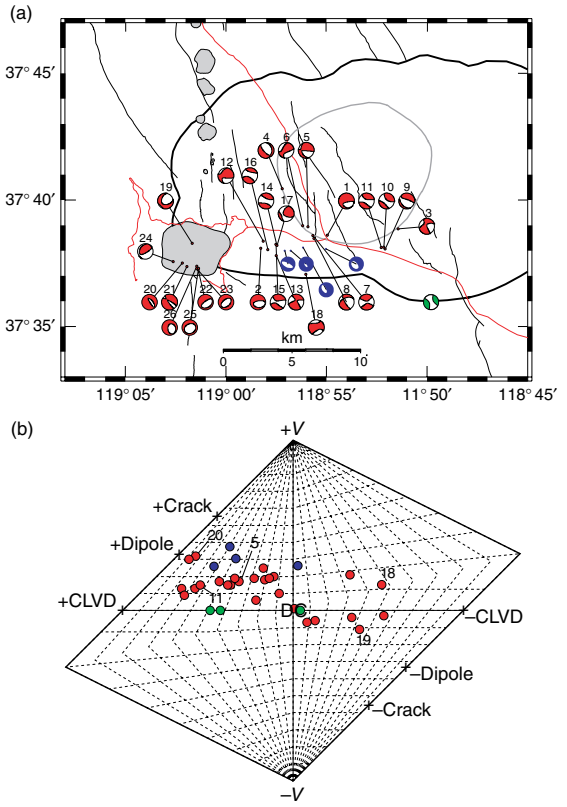

Figure 10 (a) Focal mechanism plot (upper focal hemisphere) of earthquakes in Long Valley. (b) Source-type plot of Hudson *et al*. (1989) for the same earthquakes. The vertical axis measures the size of volumetric component, and deviatoric moment tensors are located on the horizontal axis (a pure double couple at the origin). Different colors indicate mechanism solutions determined by different researchers. Adapted from Foulger GR, Julian BR, Hill DP, Pitt AM, Malin PE, and Shalev E (2004) Non-double-couple microearthquakes at Long Valley caldera, California, provide evidence for hydraulic fracturing. *Journal of Volcanology and Geothermal Research* 132: 45–71.

Kanamori *et al.* (1984). At a long-period limit, a landslide may be viewed as a sliding of a box along a slope (Hasegawa and Kanamori, 1987; Kawakatsu, 1989), and its single force equivalence may be obvious. Kawakatsu (1989) developed a centroid single force (CSF) inversion method, an extension of the centroid moment tensor (CMT) inversion method of Dziewonski *et al.* (1981) to include single force components, and applied it successfully to several landslide/slump events recorded by global seismic networks. Ekström *et al.* (2003) applied the CSF inversion to 'glacial earthquakes' observed in southern Alaska, and showed that they are represented by stick-slip, downhill sliding of a glacial ice mass which takes about 30–60 s in duration.

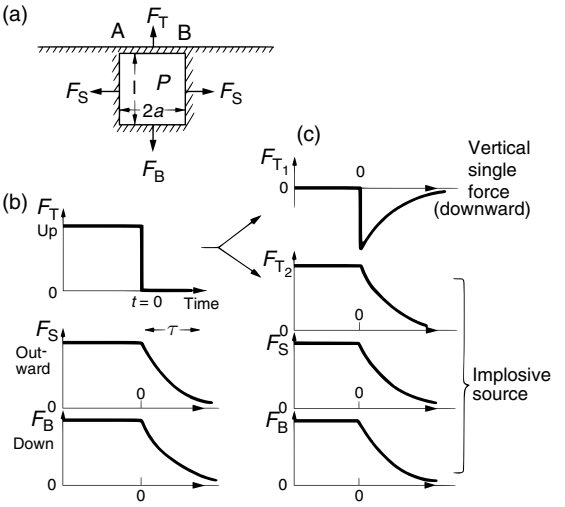

Figure 11 A force system equivalent to a volcanic eruption. (a) A pressure release model for a volcanic eruption. (b) Forces acting on the top, side, and bottom walls. (c) Decomposition of the force to a vertical single force and an implosive force. Adapted from Kanamori H, Given JW, and Lay T (1984) Analysis of seismic body waves excited by the Mount St. Helens eruption of May 18, 1980. *Journal of Geophysical Research* 89: 1856–1866.

Kanamori *et al.* (1984) also suggested that an equivalent force system for a volcanic eruption can be decomposed into a vertical downward single force and an isotropic moment tensor (**Figure 11**). A single force source may be also realized when high-viscous magma flows along a narrow conduit, as suggested by Ukawa and Ohtake (1987) to explain the deep monochromatic low-frequency (1 Hz) event observed beneath Izu-Oshima Volcano, Japan, about 1 year prior to the 1986 eruption. Chouet *et al.* (2003) also suggested that a piston-like rise of a slug of gas in the conduit produced observed single force components in the long-period signals associated with explosions in Stromboli Volcano, Italy.

4.13.3.4 Waveform Analysis of Volcanic Seismic Sources

The long-period part of volcanic seismic signals has been recorded by seismic networks of regional and/or global scales. One of the advantages of using such long-period signals is that waveform analysis to infer excitation mechanisms can be easily performed compared to short-period seismograms. As mentioned, Kanamori and Given (1982) modeled the long-period seismic signals accompanied with the eruption of the Mt. St. Helens in 1980 recorded at stations of the

global seismic networks. They showed that the single force mechanism can explain the radiation pattern of long-period surface waves, and attributed it to the gigantic mass movement of the volcano edifice due to a landslide. Kanamori *et al.* (1984) also analyzed the long-period body waves generated by the same eruption, and showed that vertical single forces due to the depressurization of the magma chamber explain the data. With these two single force mechanisms, they could vividly picture what had occurred during the whole sequence of the eruption. These two studies initiated the applications of 'long-period seismology' to study volcanic activities.

For long-period seismic signals, it is often appropriate to treat the source originating from a point in space. Then seismic wave field u_n ($\mathbf{x}$, t) may be written as

$$u_n(\mathbf{x}, t) = G_{np,q}(\mathbf{x}, \mathbf{x}_0, t) * M_{pq}(t) + G_{np}(\mathbf{x}, \mathbf{x}_0, t) * F_p(t)$$

where $M_{pq}(t)$ and $F_p(t)$ denote a moment tensor and single-force source time function at $\mathbf{x}_0$, respectively, and G_{np} ($\mathbf{x}$, $\mathbf{x}_0$, t) and $G_{np,q}$ ($\mathbf{x}$, $\mathbf{x}_0$, t) respectively represent Green's function and its spatial derivative (e.g., Aki and Richards, 2002); the asterisk denotes convolution, and the summation convention for repeated indices is assumed. Knowing the Earth structure (i.e., knowing the Green's function) and having enough waveform data, it is then possible to solve for the time history of general seismic sources, $M_{pq}(t)$ and $F_p(t)$.

Takeo *et al.* (1990) extended the waveform moment tensor inversion technique commonly used in the analysis of far-field records in earthquake seismology (e.g., Kikuchi and Kanamori, 1982) to volcano seismology by including the single force contribution. They applied it to the records observed in a lava drain-back stage of the 1987 eruption of Izu-Oshima Volcano, Japan, and showed that the resolved vertical single forces with opposing directions are due to a rapid collapse of overloading lava into the deeper vent. Ohminato *et al.* (1998) applied a similar technique to near-field broadband records observed at Kilauea Volcano, USA, and showed that long-period signals can be explained by a subhorizontal crack which periodically injects magma into a larger reservoir. Chouet *et al.* (2003, 2005) and Ohminato (2006) further incorporated the effect of complex topography of volcanic edifice that may significantly distort seismic signals observed in the near-field by calculating Green's functions using the finite difference scheme developed by Ohminato and Chouet (1997).

The general source analysis for long-period signals using moment tensor and single force has become common in seismological studies of volcanic activities. Examples of such studies include Mt. St. Helens (Kanamori and Given, 1982; Kanamori *et al.*, 1984; Kawakatsu, 1989); Long Valley (Julian, 1983; Aki, 1984; Wallace, 1985; Dreger *et al.*, 2000); Kilauea, Hawaii (Eissler and Kanamori, 1987; Ohminato *et al.*, 1998), USA; Asama (Takeo *et al.*, 1984; Ohminato *et al.*, 2006); Izu-Oshima (Takeo *et al.*, 1990); Sakurajima (Uhira and Takeo, 1994); Unzen (Yamasato *et al.*, 1993; Uhira *et al.*, 1994b); Ito-oki (Takeo, 1992); Tori-shima (Kanamori *et al.*, 1993), Japan; Iceland (Julian *et al.*, 1997; Nettles and Ekström, 1998); Stromboli, Italy (Chouet *et al.*, 2003); and Popocatépetl, Mexico (Chouet *et al.*, 2005). Applications of such analysis techniques for shorter-period (~1 s) near-field records obtained at volcanoes are also becoming available (e.g., Uhira *et al.*, 1994a; Nishimura *et al.*, 1995; Aoyama and Takeo, 2001; Nakamichi *et al.*, 2003; Nakano *et al.*, 2003; Ohminato, 2006; Kumagai *et al.*, 2005).

4.13.4 Physical Mechanisms for Volcanic Seismic Signals

The presence of ample fluid (gas, vapor, magma, or their mixtures) in volcanic edifice introduces an additional interesting class of vibration/wave phenomena to the well-studied elastic formulations. For example, the so-called 'crack wave', which is introduced by Chouet (1986) to explain the low-frequency nature of volcanic events, may be understood as a part of a class of waves due to solid/fluid coupling. Julian (1994) showed that the nonlinear effect of such solid/fluid coupling due to fluid flow transient can generate a wide variety of waveforms which have similar characteristics as volcano seismic signals. This section summarizes some such topics, relevant to generation of volcano-specific seismic signals.

4.13.4.1 Slow Waves in Solid/Fluid Composite

There exists a class of waves in the two-phase system of a solid–liquid composite that travel slower than any of the sound velocities of the pure material constituting the two-phase system (i.e., the wave speed

can be slower than that of the liquid phase). These waves include the tube wave (Biot, 1952), so-called Biot's slow wave in a porous medium (Biot, 1956), so-called crack wave (Chouet, 1986; Ferrazzini and Aki, 1987), and waves in solid–liquid alternating layers (Schoenberg and Sen, 1983) (Rayleigh wave and Stoneley wave may also be included in the same class, considering that in the high-frequency limit, all the above slow waves have the same characteristics as an interface wave).

The simplest (and the most relevant to volcano seismology) example of slow waves may be the plane wave propagation in a medium which consists of a fluid layer sandwiched by two elastic half-spaces studied by Ferrazzini and Aki (1987), who investigated the physical basis of the crack wave found by Chouet (1986). Here we follow Yamamura (1997) to formulate the problem.

Following Aki and Richards (2002, p. 263), we first express a plane-wave solution propagating parallel to the fluid layer as

$$\begin{pmatrix} u \\ w \end{pmatrix} = \begin{pmatrix} r_1(z) \\ \mathrm{i}r_2(z) \end{pmatrix} e^{\mathrm{i}(kx-\omega t)} \qquad [18]$$

where u and w are respectively the displacements for x- and z-directions. The frequency domain equation of motion in x-direction for the fluid layer may then be written as

$$-\omega^2 \rho_\mathrm{f} r_1 = -k^2 \kappa_\mathrm{f} r_1 - k\kappa_\mathrm{f} \frac{\partial r_2}{\partial z} \qquad [19]$$

where ρ_f and κ_f denote density and bulk modulus of the fluid, respectively. Integrating [19] over the thickness of the fluid layer (i.e., z-direction) with appropriate boundary conditions (e.g., free-slip condition at the solid/fluid interface), we get the following expression:

$$-\omega^2 \rho_\mathrm{f} \int_0^H r_1 \mathrm{d}z = -k^2 \kappa_\mathrm{f} \int_0^H r_1 \mathrm{d}z - k\kappa_\mathrm{f} r_2(H) \qquad [20]$$

where we assume a symmetric solution for the z-dependency (Ferrazzini and Aki, 1987) and the thickness of the fluid layer $2H$.

Equation [20] clearly demonstrates the role of the interface: without the last term $r_2(H)$, [20] indicates the averaged displacement in the fluid layer traveling with its own sound velocity; that is, the term represents the way the fluid layer is coupled with the surrounding elastic half-space. If we further rewrite [20] as

$$-\omega^2 \rho_\mathrm{f} \int_0^H r_1 \mathrm{d}z = -k^2 \kappa_\mathrm{f} \left[1 + \frac{1}{k} \frac{r_2(H)}{\int_0^H r_1 \mathrm{d}z} \right] \int_0^H r_1 \mathrm{d}z \qquad [21]$$

it is seen that

$$\kappa_\mathrm{f}^\mathrm{e} \equiv \kappa_\mathrm{f} \left[1 + \frac{1}{k} \frac{r_2(H)}{\int_0^H r_1 \mathrm{d}z} \right]$$

represents the effective bulk modulus for the fluid layer; when $\kappa_\mathrm{f}^\mathrm{e} < \kappa_\mathrm{f}$, that is,

$$\frac{r_2(H)}{\int_0^H r_1 \, \mathrm{d}z} < 0 \qquad [22]$$

the corresponding traveling wave has a smaller wave speed relative to the sound velocity; thus we have a slow wave. The condition [22] is satisfied if the denominator and numerator have an opposite sign to each other. This makes quite good sense intuitively; when the fluid 'tries' to contract (or expand) as a passage of the wave, due to the 'elastic coupling' along the solid/fluid boundary, there exists a solution in which the solid behaves out of phase to the fluid to expand (contract), deforming the boundary in such a way that fluid 'feels' easy to contract (expand), compared to the single-phase case; that is for a given amount of displacement in the propagation direction, the actual pressure increment of the fluid phase becomes lower than that of the pure fluid case (**Figure 12**). The net effect of this elastic coupling

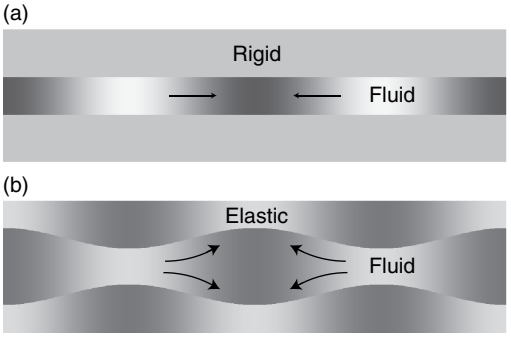

Figure 12 Conceptual image of the slow wave in solid/fluid composites. Out-of-phase motion of the solid (b) lowers the 'effective bulk modulus' of the fluid, and as a result the wave speed becomes slower than that in the pure fluid (a).

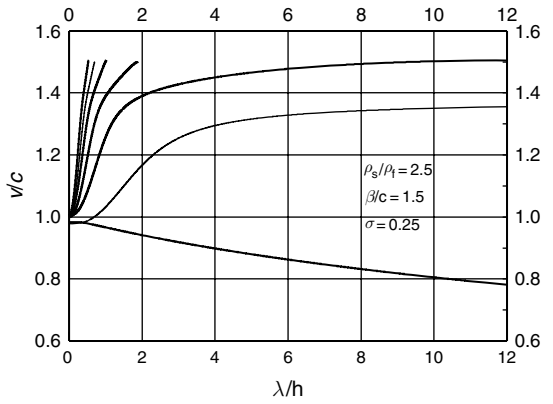

Figure 13 Phase velocity divided by the acoustic velocity of the fluid is plotted as a function of the wavelength divided by the fluid layer thickness. The fundamental branch having a phase velocity below 1 corresponds to the slow wave. Adapted from Ferrazzini V and Aki K (1987) Slow waves trapped in a fluid-filled infinite crack: Implication for volcanic tremor. *Journal of Geophysical Research* 92: 9215–9223.

is to reduce the 'effective bulk modulus' (i.e., the restoring force) of the fluid, and as a result the wave speed becomes slower than that of the pure fluid; stronger the elastic coupling, slower the wave speed (**Figure 13**).

This kind of the out-of-phase condition is satisfied by other slow waves such as Biot's slow wave in porous medium (Biot, 1956), and waves in solid/fluid alternating layers (Schoenberg and Sen, 1983). Indeed, using the argument presented above, Yamamura (1997) was able to derive a similar set of equations to describe the elastic coupling for the Schoenberg's problem to those Biot's equations of motion, and suggested that all these slow waves have a similar characteristic as an interface wave, and that in the short-wavelength limit they reduce to the Stoneley wave.

4.13.4.2 Resonating Sources: A Crack

The presence of regularly spaced spectral peaks often observed in volcanic seismic signals immediately reminds us of the presence of resonators within the volcanic edifice filled with volcanic fluid. To quantitatively model the volcanic tremor observed at Kilauea, Hawaii, Aki *et al.* (1977) considered fluid-filled tensile cracks as the most plausible resonating sources. Using two-dimensional finite difference method, they computed the dynamics of a series of fluid-filled cracks connected by narrow channels which are excited by jerky extension/opening of channels due to excess fluid pressure. Although their model offers both the driving force and the geometry adequate for the magma transport beneath active volcanoes, the fluid inside the crack acts passively like a cushion so that the stress at the crack wall depends only on local displacements of the crack wall; the fluid also dose not support the propagation of pressure perturbation caused by the deformation of the crack wall. To assess active roles of the fluid, Chouet and Julian (1985) extended Aki *et al.*'s model, and investigated dynamic interaction between fluid and elastic solid inside and outside a two-dimensional crack by solving equations for the elastic solid and the fluid simultaneously. The model was further extended to three-dimension by Chouet (1986).

Chouet's three-dimensional model consists of a single isolated fluid-filled crack in an infinite elastic solid body, and no external mass transfer into and/or out of the crack is taken into consideration. In the model, the thickness of the crack d is assumed to be much smaller than the wavelength of interest, and thus the motion of the fluid inside the crack is treated as two-dimensional. Assuming Poisson's ratio to be 0.25 (i.e., $\lambda = \mu$) and taking L and L/α as the characteristic length and time, where L and α are the length of the crack and the P wave velocity in the solid, the response of the crack is calculated by solving following dimensionless equations simultaneously with boundary conditions at the crack surface and perimeters:

$$\begin{aligned}
\text{Solid:}\quad & \frac{\partial \tilde{v}_i}{\partial \tilde{t}} = \frac{1}{3}\frac{\partial \tilde{\tau}_{ik}}{\partial \tilde{x}_k} \\
& \frac{\partial \tilde{\tau}_{ij}}{\partial \tilde{t}} = \frac{\partial \tilde{v}_k}{\partial \tilde{x}_k}\delta_{ij} + \frac{\partial \tilde{v}_i}{\partial \tilde{x}_j} + \frac{\partial \tilde{v}_j}{\partial \tilde{x}_i} \\
\text{Fluid:}\quad & \frac{\partial \tilde{U}_l}{\partial \tilde{t}} = -\frac{1}{3}\frac{\rho}{\rho_f}\frac{\partial \tilde{P}}{\partial \tilde{x}_l} \\
& \frac{\partial \tilde{P}}{\partial \tilde{t}} = -\frac{\kappa_f}{\mu}\frac{\partial \tilde{U}_m}{\partial \tilde{x}_m} - 2\frac{\kappa_f}{\mu}\frac{L}{d}\tilde{v}_z \\
& (\tilde{x} = x/L,\ \tilde{t} = t\alpha/L)
\end{aligned} \qquad [23]$$

In these equations, the quantities with tilde represent dimensionless ones, and $\tilde{v}$ and $\tilde{\tau}$ are the velocity and the stress of the solid; $\tilde{U}$ and $\tilde{P}$ are the velocity and the pressure of the fluid, ρ and ρ_f are the density of the solid and the fluid, μ and κ_f are the rigidity of the solid and the bulk modulus of the fluid, respectively. As shown in [23], the behavior of fluid-filled crack critically depends on a nondimensional parameter $c = \kappa_f/\mu \cdot L/d$, which was first introduced by Aki *et al.* (1977) and named as 'crack stiffness' by Chouet (1986).

Synthetic seismograms calculated by the fluid-filled model show strong similarities to observed volcanic signals in terms of both peaked spectra and long-lasting oscillations, and demonstrated the importance of active participation of fluids in source dynamics generating volcanic seismic signals. These studies include the interpretations of volcanic signals observed at Redoubt, Alaska (Chouet *et al.*, 1994); Galeras, Colombia (Gil Cruz and Chouet, 1997, **Figure 14**); Kusatsu-Shirane, Japan (Nakano *et al.*, 1998; Kumagai *et al.*, 2002); Kilauea, Hawaii (Kumagai *et al.*, 2005); and other volcanoes.

Kumagai and Chouet (1999, 2000) and Morrissey and Chouet (2001) further studied the dependencies of frequencies and attenuations of crack-resonant oscillations on the properties of fluid in more detail using various models of fluid–gas mixtures and fluid–particle mixtures, and demonstrated that the fluid properties and compositions can be estimated from frequencies and attenuations of observed signals. These results are used to assess the change of magmatic and hydrothermal system beneath the volcano at Kusatsu-Shirane, Japan (Kumagai *et al.*, 2002; **Figure 15**) and Tungurahua, Ecuador (Molina *et al.*, 2004).

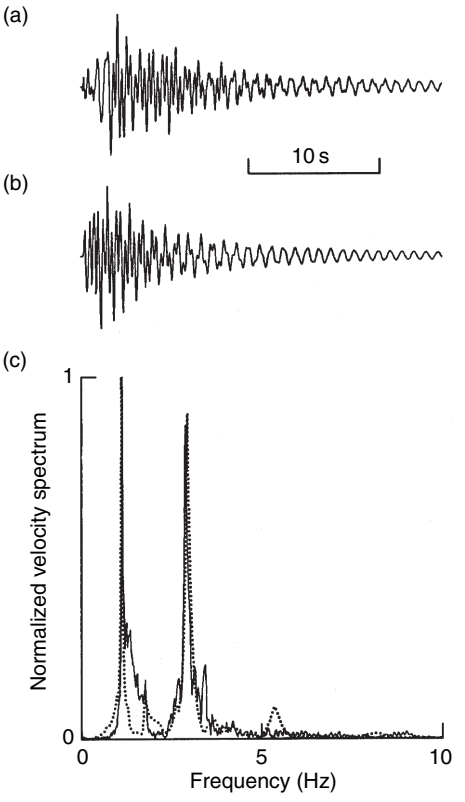

Figure 14 Example of the application of the fluid-filled crack model: (a) Vertical velocity seismogram observed at Galeras Volcano, Colombia. (b) Synthetic waveform obtained from the fluid-filled crack model. (c) Spectrum of observed data (thin line) and synthetic data (dotted line). Adapted from Chouet B (1996a) Long-period volcano seismicity: Its source and use in eruption forecasting. *Nature* 380: 309–316.

4.13.4.3 Other Resonating Sources

Although the presence of regularly spaced spectral peaks may not straightforwardly warrant the presence of a resonator (Julian, 1994), it seems indeed natural to think of such presence like a crack as a dike, a cylinder as a conduit, and a sphere as a magma chamber, as they are all fundamental constituents of a volcano.

Resonators as models of the origins of volcanic seismic signals besides a crack have been suggested for a cylinder (Ferrick *et al.*, 1982; Chouet, 1985), and a sphere (Sassa, 1935; Kubotera, 1974). Crosson and Bame (1985) obtained an impulsive response of a spherical magma chamber with a spherical cavity inside. Fujita *et al.* (1995) solved eigenoscillation of a fluid sphere embedded in an infinite elastic medium. Fujita and Ida (2003) conducted a systematic survey of the geometrical effects on the eigenoscillations, and showed that the ratios of higher modes to the fundamental mode frequencies can be indicators of the geometry of the resonator. They also found a class of modes with a low attenuation named 'low-attenuation mode' (LAM), which share the similar out-of-phase characteristics of the slow waves discussed above, and suggested that LAM may be the origin of long-lasting low-frequency oscillation of volcanic seismic signals.

The complicated nature of vibrations of cylindrical conduits has been numerically studied (e.g., Neuberg *et al.*, 2000; Jousset *et al.*, 2003; Nishimura and Chouet, 2003). Neuberg *et al.* (2000) introduced a depth-dependent seismic velocity model to account for the varying gas content in the magma, and showed that a pressure change in the conduit was the most likely candidate for the physical process causing the peak-spectral shift often observed in many of volcanoes (**Figure 4**). Jousset *et al.* (2003) also showed that the end points of the conduit can act as secondary sources of volcanic seismic signals.

The excitation mechanism of these resonators is, on the other hand, not well understood. The proposed models include a jerky extension of the crack tip (Aki *et al.*, 1977), acoustic emissions from collapsing bubbles (Chouet, 1992), rapid discharge of fluids

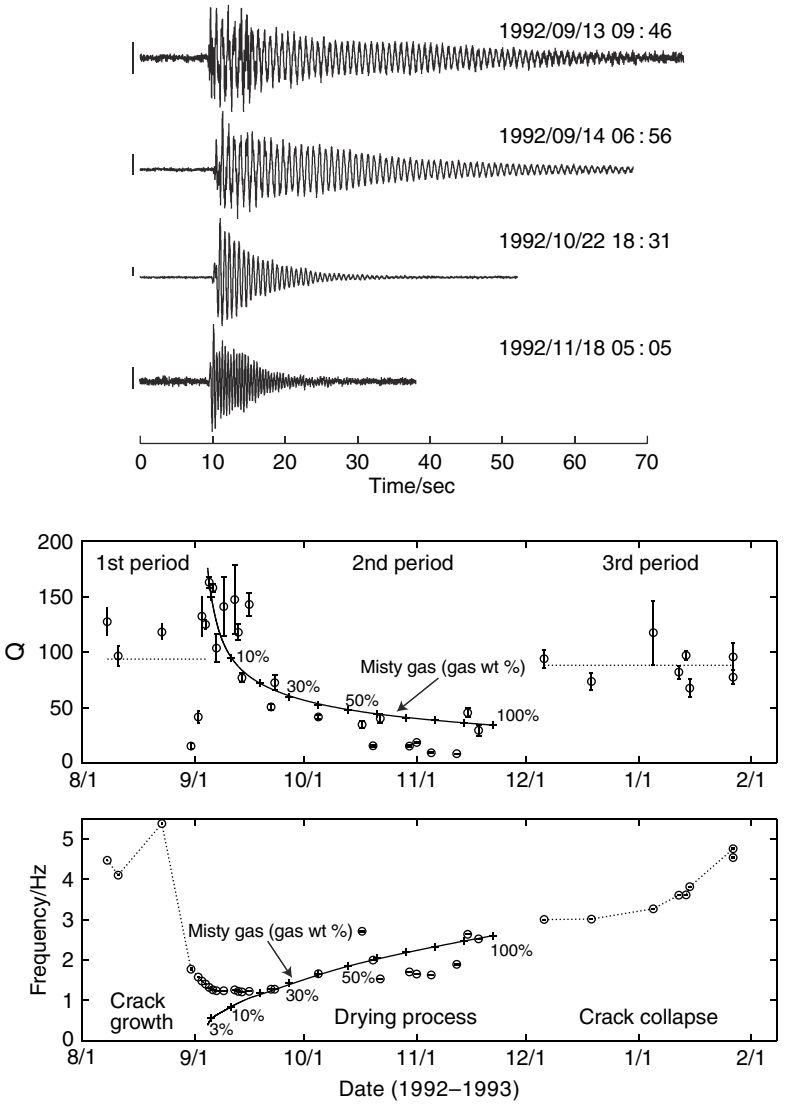

Figure 15 Temporal change of waveforms observed at Kusatsu-Shirane Volcano and the fluid properties estimated from the frequency and the attenuation of signals. From Kumagai H, Chouet B, and Nakano M (2002) Temporal evolution of a hydrothermal system in Kusatsu-Shirane Volcano, Japan, inferred from the complex frequencies of long-period events. *Journal of Geophysical Research* 107: ESE 9–1.

(Ferrick *et al.*, 1982), and a sudden pressure drop caused by unsteady choked flow (Morrissey and Chouet, 1997). Nakano *et al.* (1998) developed a method to extract the effective excitation function from seismic records based on an inhomogeneous autoregressive (AR) model of a linear dynamic system. Nakano *et al.* (2003) further extended the method to deal with the nonorthogonal nature of eigenfunctions of a resonator embedded in a rock matrix by using the biorthogonal eigenfunction expansion method of Yamamura and Kawakatsu (1998); the resolved effective excitation functions of the low-frequency events in Kusatsu-Shirane Volcano, Japan, are then modeled by the waveform inversion method of Ohminato *et al.* (1998) to obtain the moment tensor and single-force source time function, which are interpreted as a result of repeated activation of a subhorizontal crack located beneath the summit crater lake.

4.13.4.4 Flow-Induced Oscillation

Julian (1994) proposed nonlinear flow-induced oscillations in channels transporting volcanic fluid as a

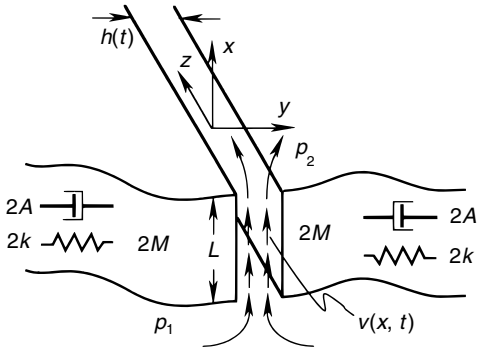

Figure 16 Lumped-parameter model of the generation of volcanic tremor. Viscous, incompressible fluid flows in *x*-direction from upstream (bottom) to downstream (top) reservoir through a channel with imperfectly elastic walls. Adapted from Julian BR (1994) Volcanic tremor: Nonlinear excitation by fluid flow. *Journal of Geophysical Research* 99: 11859–11878.

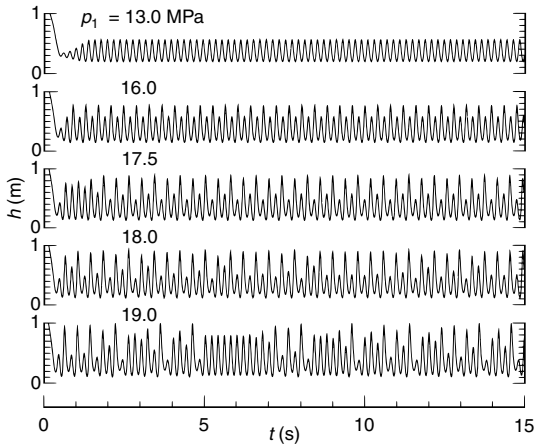

Figure 17 Synthetic tremor time series (channel thickness *h* versus time) for different values of the upstream pressure p_1. Behavior changes from a simple limit cycle (top) to chaos (bottom), with some period doubling in between. Adapted from Julian BR (1994) Volcanic tremor: Nonlinear excitation by fluid flow. *Journal of Geophysical Research* 99: 11859–11878.

possible generating mechanism for volcanic seismic signals, particularly for sustained volcanic tremors. The mechanism may have analogs such as the vibration of vocal chords, musical wind instruments, etc., and the periodic behavior, often characteristic of volcanic seismic signals, occurs without the presence of a resonator.

Figure 16 shows the simplified lumped-parameter model of the flow of a viscous fluid through a constricted channel with elastic walls. The channel walls are modeled as masses connected by a spring and dashpot to represent the effects of the elastic stiffness and radiation loss. The mechanism may be summarized as follows: an increase in a flow speed leads to a decrease in fluid pressure by the Bernoulli effect; as a result, the walls narrow the channel to constrict the flow, causing a pressure increase and forcing the channel open again; this again decreases the pressure and increases the flow speed. This positive feedback mechanism sustains the oscillation.

Julian (1994) derived a third-order nonlinear system of ordinary differential equations that describe the complete behavior of the system and may be solved numerically. The system without radiation damping exhibits two different types of behavior: oscillations that grow and approach a stable tremor-like limit cycle, and transient oscillations that decay, leading to a steady flow. Inclusion of the damping further complicates the behavior, as shown in **Figure 17**. By increasing the upstream pressure, the system experiences so-called period doubling, that is, an appearance of a subharmonic with a frequency half that of the fundamental frequency; further increase with successive period doubling eventually leads to chaotic behaviors. Julian suggests that these features resemble behavior of some of the volcanic tremors and the deep low-frequency event observed in Hawaii (Aki and Koyanagi, 1981).

Balmforth *et al.* (2005) extended Julian's treatment to include the dynamic behavior of the fluid and the elasticity of the surrounding walls, and considered the excitation of propagating waves. Their results confirm that Julian's mechanism is plausible, but the physical condition required for the instability is different. They conclude that magma itself is unlikely to generate flow-induced oscillations, but that the rapid flow through fractured rock of low-viscosity fluids exsolved from magma may. A similar flow-induced oscillation is also studied by Ida (1996) to explain the sawtooth nature of geodetic signals.

In fluid/gas two-phase system. The flow-induced oscillation described above assumes flows of a single-phase fluid. Volcanic fluids such as magma often contain ample gases, especially at a shallow depth, and it may be more reasonable to consider a flow of two-phase fluids consisting of liquid and gas phases rather than single-phase fluids as a source of volcanic seismic signals. Such a flow of liquid/gas two-phase fluid is also seen in, for example, the evaporation pipes in boiler systems, nuclear reactor cooling systems,

chemical industry equipments, and many studies have been conducted extensively in the field of engineering. These studies revealed the existence of flow-induced oscillatory phenomena, which is not observed in a flow of single-phase fluid, caused by complex interactions between two phases.

Iwamura and Kaneshima (2005) considered one of these flow-instability phenomena called 'density wave oscillation', which was originally studied in the nuclear reactor engineering, as a model of volcanic seismic signals, and evaluated the properties of generated seismic waves through a series of numerical experiments. Another kind of flow-induced oscillation in fluid/gas two-phase flows called 'pressure drop oscillation' was also invoked to interpret the cyclic tilt change observed at Miyake-jima Volcano by Fujita *et al.* (2004).

4.13.4.5 Bubble Dynamics

Gasses dissolved in magma are one of the main driving forces to cause various volcanic phenomena. The presence of gas bubbles in magma decreases the density of magma, and drives the magma ascent from the deep part of volcanoes (e.g., Wilson and Head, 1981). At shallower depths, the relatively high compressibility of bubbles contributes to the generation of oscillatory phenomena specific to volcanoes (e.g., Kieffer, 1977; Chouet, 1996a), and the transformation and the fragmentation of bubbles affect the behavior of volcanic eruptions (e.g., Alidibirov and Dingwell, 1996; Ichihara *et al.*, 2002).

In relation to volcano seismology, there are some aspects where bubbles play important roles. As described above, volcanic seismic signals are often characterized by long-lasting low-frequency oscillations with sharp spectral peaks (**Figure 1**), which are reminiscent of oscillations of some resonator filled with material with a slow acoustic velocity. Since the existence of bubbles in magma drastically changes the compressibility of magma, as pointed out by Kieffer (1977), these characteristics of volcanic seismic signals have been partly attributed to the presence of bubbles in magma. The rapid temporal changes of the observed spectral peaks (e.g., Benoit and McNutt, 1997; Neuberg *et al.*, 2000) have also been considered to reflect the change in the state of gas bubbles in volcanic conduits.

Bubbles in magma also act as an active source of seismic and acoustic signals: the bursting and the collapsing of bubbles at the lava surface preceding and/or accompanying volcanic eruptions generate acoustic pressure signals which are sometimes accompanied with seismic waves (e.g., Vergniolle *et al.*, 1996; Ripepe *et al.*, 1996); the collapse of small bubbles in hydrothermal fluids generates seismic tremors (e.g., Leet, 1988); the movement of large-scale bubbles (slugs) in magma conduit causes an exchange of their momentum with the surrounding rocks and generates seismic signals that show dominant single force components (e.g., Ohminato *et al.*, 1998; Ripepe and Gordeev, 1999; Chouet *et al.*, 2003, 2005); the forced oscillations of bubbles by strain waves can rapidly pump dissolved volatiles into bubbles by a mechanism called 'rectified diffusion' and the resultant pressure increase may trigger volcanic activities (e.g., Brodsky *et al.*, 1998; Ichihara and Brodsky, 2006).

In spite of the difference in their generation mechanisms and resultant phenomena, all of these phenomena are the manifestations of passive and active processes in which the thermochemical energy and/or the gravitational energy of the volcanic fluids are transduced into seismic/acoustic energy. The quantitative understanding of the behavior of bubbles, thus, is a critical key to elucidate the dynamics of volcanic phenomena.

4.13.5 Observation and Analysis Aspects

In addition to the conventional monitoring of active volcanoes using short-period seismometers and geodetic instruments, the digital era has brought new powerful components to seismometry of active volcanoes; broadband and array seismometries may be two of the most notable developments.

4.13.5.1 Broadband Seismometry

The first broadband seismic observation at an active volcano was conducted by Sassa (1935), who installed Wiechert horizontal-component seismographs (pendulum period $T_0 = 10.0\,\mathrm{s}$) and vertical ones ($T_0 = 4.6\,\mathrm{s}$), Galitzin seismographs ($T_0 = 8.0\,\mathrm{s}$), and short-period seismographs ($T_0 = 0.55\,\mathrm{s}$) at Aso Volcano. Summarizing the subsequent observations in a period of several years, Sassa classified volcanic seismic signals of Aso into 'eruption earthquakes' and four different kinds of tremors: periods of 0.2, 0.4–0.6, 0.8–1.5, and 3.5–8.0 s. The observation of these tremors in the wide frequency band ranging from 0.2 to 8.0 s clearly demonstrates the efficacy of broadband

seismometry at active volcanoes. Since Sassa's pioneering work, until 1990s (when it has become much easier to install portable broadband instruments), there have not been many published reports on attempts to observe long-period volcanic seismic signals except for a few cases. For example, Seidl *et al.* (1981) installed broadband seismometers at Etna, Italy, and observed 4–5 s period signals, which they suggested as one of the fundamental peaks of the Etna tremors.

Examples of deployments of the current-generation broadband seismometers are now plentiful, for example, Sakurajima (Kawakatsu *et al.*, 1992, 1994) Unzen (Yamasato *et al.*, 1993; Uhira *et al.*, 1994b) Aso (Kaneshima *et al.*, 1996; Yamamoto *et al.*, 1999; Kawakatsu *et al.*, 2000; Legrand *et al.*, 2000) Satsuma-Iwojima (Ohminato and Ereditato, 1997; Ohminato, 2006) Iwate (Nishimura *et al.*, 2000); Miyake-jima (Kumagai *et al.*, 2001; Fujita and Ida, 2003), Usu (Yamamoto *et al.*, 2002) Bandai (Nishimura *et al.*, 2003) Hachijo-jima (Kumagai, 2006) Asama (Ohminato *et al.*, 2006), Japan; Stromboli (Dreier *et al.*, 1994; Falsaperla *et al.*, 1994; Neuberg *et al.*, 1994; Chouet *et al.*, 2003), Italy; Semeru (Hellweg *et al.*, 1994) Merapi (Hidayat *et al.*, 2000, 2002), Indonesia; Arenal (Hagerty *et al.*, 2000), Costa Rica; Kilauea (Dawson *et al.*, 1998; Ohminato *et al.*, 1998; Almendros *et al.*, 2002a), Long Valley (Hill *et al.*, 2002; Hill and Prejean, 2005), Mt. St. Helens (Waite *et al.*, 2005), USA; Erebus (Rowe *et al.*, 1998, 2000; Aster *et al.*, 2003), Antarctica; Popocatépetl (Arciniega-Ceballos *et al.*, 1999, 2003; Chouet *et al.*, 2005), Mexico; Karymsky, Russia; and Sangay (Johnson and Lees, 2000), Ecuador. A variety of long-period volcanic seismic signals have been observed at different volcanoes.

Besides the advantages already mentioned, the long-period seismic wavefield observed with a broadband seismic network may be used to directly monitor the activity of a volcano. Dawson *et al.* (2004) implemented the radial semblance method of Kawakatsu *et al.* (2000; originally called 'waveform semblance') for the near real-time monitoring of the activities at the shallow magmatic conduit in Kilauea Volcano, Hawaii (**Figure 18**). Similarly, the moment tensor and single-force source real-time monitoring should be possible using a grid-based method as suggested by Kawakatsu (1998) and implemented at the Earthquake Research Institute of the University of Tokyo for the real-time seismicity monitoring, and as recently realized at Stromboli Volcano (Auger *et al.*, 2006).

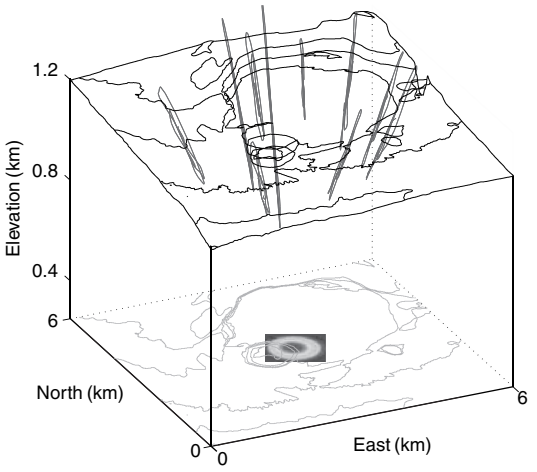

Figure 18 Particle motions recorded by the network during a 1 min long window of long-period signal. The area with bright colors with high semblance values indicates the source region. Adapted from Dawson P, Whilldin D, and Chouet B (2004) Application of near real-time radial semblance to locate the shallow magmatic conduit at Kilauea Volcano, Hawaii. *Geophysical Research Letters* 31: L21606.

4.13.5.2 Array Analysis

To locate the source of volcanic signals, various kinds of methods have been applied to the analyses of observed data. Classical hypocenter determination methods using phase arrivals have been applied to signals observed around active volcanoes and used to predict the eruptions (e.g., Scarpa and Tilling, 1996). More advanced methods such as relative hypocenter determination using the cross-spectral and the double difference have also been applied to volcanic earthquakes and have revealed vivid images of volcanic activities like the transportation of magma beneath active volcanoes (e.g., Hayashi and Morita, 2003).

Nevertheless, there still exist some specific issues to be explored in the analyses of volcanic signals due to complex source processes and complicated wave propagations in inhomogeneous structures. Lack of clear phases and relatively low dominant frequencies of, for example, low-frequency events and volcanic tremors make the direct application of the conventional hypocenter determination means rather difficult.

In the past decade, these difficulties have been partly overcome by the use of seismic arrays. In array observations, seismometers are placed at short distance intervals (a few tens to hundreds of meters), and thus

the wave properties of the incident waves can be examined by extracting coherent portion of the signals using the array data. Recent advance in portable instrumentation enables us to observe volcanic signals close to their sources with dense arrays and sheds new light on the understanding of the processes through the precise determination of location and distribution of volcano seismic sources. For example, the MUSIC (MUltiple SIgnal Classification) technique (Schmidt, 1986; Goldstein and Archuleta, 1991) has been applied to the analyses of the array data observed at Kilauea, Hawaii (e.g., Goldstein and Chouet, 1994; Almendros *et al.*, 2002a, 2002b; **Figure 19**), and at Stromboli, Italy (e.g., Chouet *et al.*, 1997), and revealed magmatic and hydrothermal activities beneath the volcanoes. Other array analysis techniques have been also applied to constrain the source locations and properties of volcanic signals (e.g., Gordeev *et al.*, 1990; Ibanez *et al.*, 2000).

Seismic arrays have also been used to constrain the shallow structure of volcanoes that is indispensable for the quantitative volcano seismology. Here, the wavefield observed by a seismic array is treated as a stationary stochastic one in time and space, and the statistical correlation method originally proposed by Aki (1957) is applied to the data to determine the wave properties such as wave types and phase velocities (e.g., Ferrazzini *et al.*, 1991; Metaxian and Lasage, 1997; De Luca *et al.*, 1997; Chouet *et al.*, 1998; Saccorotti *et al.*, 2001a).

4.13.6 Models for Volcanic Seismic Signals

Although the basic governing physics, some of which have been discussed above, are common, and the methods of data acquisition and analyses employed

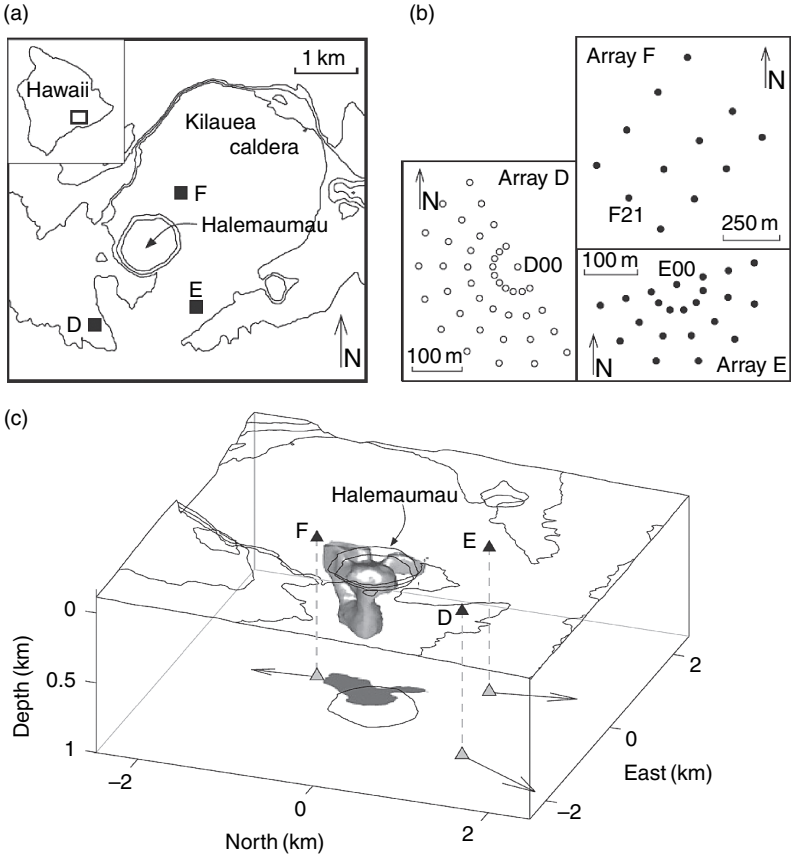

Figure 19 Example of array observation. (a) and (b) Configuration of the array observation at Kilauea, Hawaii. (c) Source location of the seismic signals obtained by array analyses. The arrows represent the apparent slowness vectors determined by frequency-slowness analyses, and the gray region is the estimated source region. Adapted from Almendros J, Chouet B, Dawson P, and Huber C (2002b) Mapping the sources of the seismic wavefield at Kilauea Volcano, Hawaii, using data recorded on multiple seismic antennas. *Bulletin of the Seismological Society of America* 92: 2333–2351.

may be the same, actual phenomena that we observed at volcanoes are different from one volcano to another. To appreciate the diversity, some of the well-studied volcanoes are reviewed. Since the names of volcanic seismic events sometimes differ from one volcano to another due to the difference in conventions as described in 'Terminology', in this section, we keep common terminology locally used at each volcano, and not necessarily follow the conventional classification of periods in earthquake seismology.

4.13.6.1 Aso

Aso Volcano is one of the most active volcanoes in Japan. It has erupted in Strombolian style repeatedly with intervals of 5–10 years, and recent activities take place at the youngest central cone which is composed of seven craters aligned northwest–southeast direction with a length of 1 km. The current eruptive activities have occurred at the first crater located at the northernmost of the chain of the craters.

Among the volcanic tremors observed by Sassa (1935), the most remarkable one is the volcanic microtremor of the second kind for its extraordinary long-period (7.5 s) and its highly repetitive occurrence. Observations using modern broadband seismometers revealed that the fundamental period of the long period tremor (hereafter LPT) is 15 s (Kaneshima *et al.*, 1996; Kawakatsu *et al.*, 2000), and that the second-kind tremor of Sassa is the higher mode of LPTs. The characteristics of LPTs are summarized as follows: (1) continually emitted from the volcano regardless of surface activity; (2) spectra show several common spectral peaks which align with almost equal spacing (15, 7.5, 5, 4 s); (3) decay fairly fast and the duration is only a few cycles; and (4) often accompanied with short-period tremors.

Kaneshima *et al.* (1996) and Kawakatsu *et al.* (2000) deployed a broadband seismic network in 1994 and analyzed the waveforms of the LPTs and those associated with phreatic eruptions which ejected composite of mud and water (**Figure 6**). They concluded that the sources of both phenomena are located a few hundred meters southwest of the first crater and at a depth of 1–1.5 km below ground surface. They further performed a source mechanism inversion of LPTs, and obtained a volumetric source mechanism which can be decomposed into an isotropic and a vertical tensile crack components (Legrand *et al.*, 2000). The detail of the tensile crack component was further studied by Yamamoto *et al.* (1999) using the data obtained by a dense broadband observation. Analyzing the spatial distribution of the signal amplitudes of LPTs (**Figure 20**), they revealed the existence of a crack-like conduit whose strike and width are almost the same as those of the chain of craters; the crack extends nearly vertically from a depth of 300–400 m below the surface to a depth of about 2.5 km, as illustrated in **Figure 21**. This observation revealed that the chain of craters is simply a surface expression of a buried crack-like conduit.

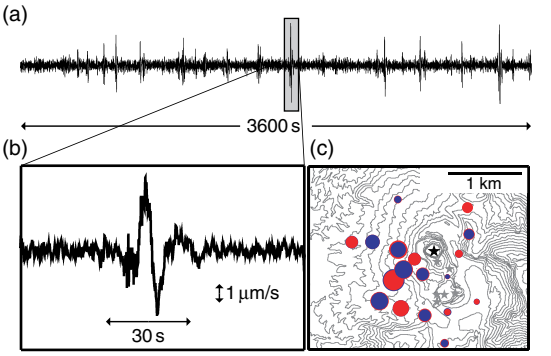

Figure 20 (a) A vertical-component broadband velocity seismogram observed at a distance of 1.5 km. Spike-like signals are LPTs. (b) Close-up view of an LPT. (c) Amplitude variation of LPTs.

The physical properties of the crack-like conduit were studied by Yamamoto (2005), who applied a boundary integral method to the oscillation of a fluid-filled crack with slits at the edges, which allow the fluid to escape, as an extension of Chouet's closed crack model (Chouet, 1986). He demonstrated that the spectral characteristics of LPTs (mode frequencies, spacing, and attenuation) can be explained by the oscillation of a 25 m thick crack-like conduit filled with gas–ash mixture. The existence of a crack-like conduit is also supported by other studies such as a reflection study by Tsutsui and Sudo (2004), and the crack-like conduit is considered as a subsurface path connecting a postulated magma chamber at a depth of around 5 km (Sudo and Kong, 2001) and the surface craters. The nature of other short-period seismic signals with a period of about 0.5 s and a period of around 0.4–0.1 s has been also studied with modern digital data obtained by dense observations using short-period seismometers (Yamamoto, 2005; Takagi *et al.*, 2006).

Figure 21 schematically summarizes the system beneath Aso Volcano that has been revealed by seismological analyses. Such a line of volcanic conduit

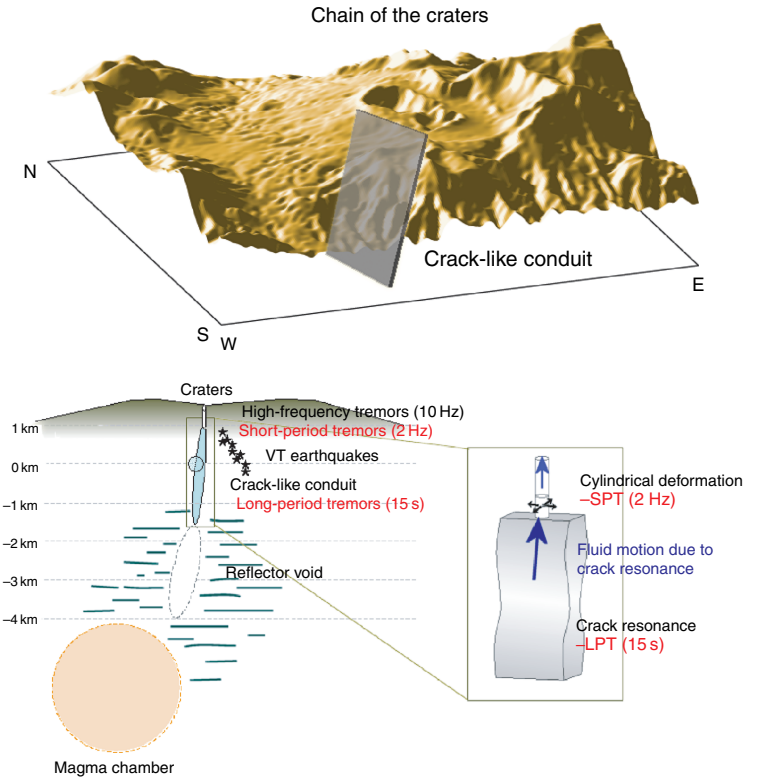

Figure 21 Image of crack-like conduit model. The crack is almost parallel to the chain of craters and the extension of the crack meets the active fumarole at the surface.

systems connecting the magma chamber and the ground surface has not been detected at any other active volcano in the world. Considering that the various volcanic signals are manifestations of dynamic interactions between volcanic fluids and volcanic edifice in the conduit system, Aso Volcano appears to be one of the best fields to study the dynamic behavior of volcanic fluid system beneath active volcanoes.

4.13.6.2 Kilauea

The Hawaiian volcanoes have been produced by the hot spot which is presently beneath the Hawaii island. The volcanoes primarily erupt basaltic magma, and the relatively low viscosity of the magma yields gentle slope of the edifices. Kilauea is the youngest and southeasternmost volcano on the Hawaii island, and it is located at the splitting point between the South-West Rift Zone and the East Rift Zone. Owing to the high level of activities and easy access to it, Kilauea may be the best-studied volcano in the world. A magma-rising system from mantle through narrow pipe-like conduit located beneath the volcano, for instance, was detected by the analyses of spatial distribution of VT earthquakes (e.g., Klein and Koyanagi, 1989), and gives a rough image of the deep magma transport and storage system beneath the volcano (**Figure 22**).

The magma transport system at shallower depths has been also studied using broadband seismic networks and short-period seismic arrays. Performing the moment tensor inversions of broadband data, Ohminato *et al.* (1998) revealed that the source of the very-long-period (VLP; 5–10 s) signals associated with a magmatic activity in 1996 is a crack-like magma pathway at a depth of 1 km, which acts like a buffer for surging magma from beneath summit of Kilauea to the East Rift Zone. Their analyses suggest that ~1000–4000 m^3 of magma is injected into the crack during a slow (1–3 min) accumulation phase, and it is ejected from the crack toward the East Rift Zone during a rapid (5–10 s) deflation phase, which together produce a sawtooth-like displacement signal shown in **Figure 23**. Dawson *et al.* (1998) also analyzed VLP signals observed in 1997, and concluded that the source location is almost

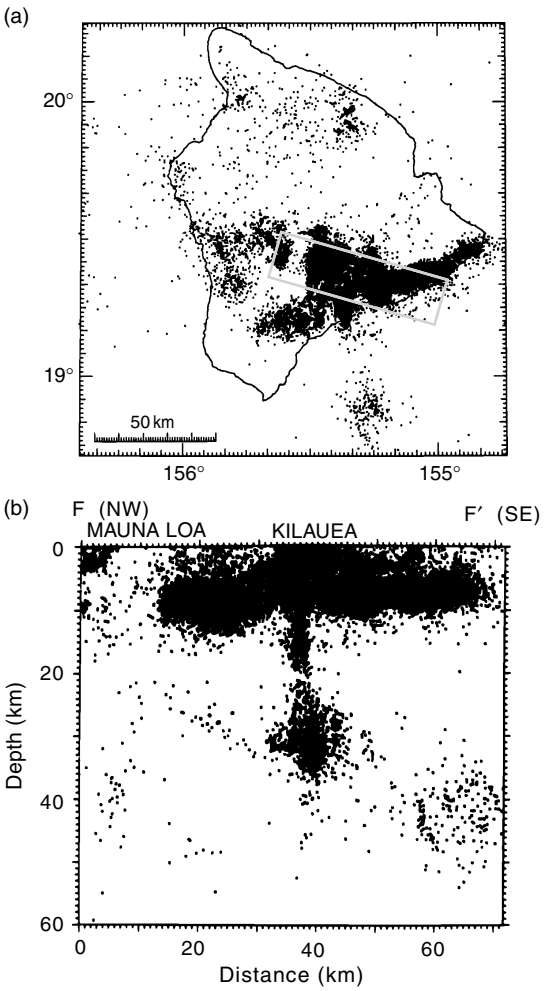

Figure 22 Seismicity of Hawaii. (a) Hypocenters of shallow earthquakes during the period 1970–84. (b) Cross section through Kilauea and Mauna Loa for earthquakes during 1970–83. The area of the cross section is that delimited by the box in the top panel. Adapted from Klein FW and Koyanagi RY (1989) The seismicity and tectonics of Hawaii. In: *The Geology of North America*, Vol. N, The Eastern Pacific Ocean and Hawaii, pp. 238–252. Geological Society of America.

the same as that determined by Ohminato *et al.* (1998), although the source mechanism is different.

The source of long-period (LP; 1–2 s) signals, on the other hand, is determined using seismic array data (e.g., Saccorotti *et al.*, 2001b; Almendros *et al.*, 2001), and the hypocenter of LP signals is located directly above the source of VLP signals. Kumagai *et al.* (2005) analyzed the source mechanism of LP signals, and imaged an expansion and contraction of a nearly horizontal crack through the moment tensor inversions. Based on the fluid-filled crack model developed by Chouet (1986), they further suggest that LP signals represent a resonance of a hydrothermal crack containing bubbly water and/or steam, and that the heat from the underlying magma conduit (VLP source) may cause the pressurization of hydrothermal fluid in the crack and trigger these LP signals. Other geophysical observations, such as a positive correlation between summit SO_2 emissions and the shallow seismicity which was pointed out by Sutton *et al.* (2001), also suggest the interaction between magmatic and hydrothermal systems at the shallow part of the volcano.

These results indicate that the detailed quantitative analyses of volcanic seismic signals are critically important for a better understanding of volcanic processes, and such analyses may be crucial steps toward eruption prediction and the assessment of volcanic hazards.

4.13.6.3 Miyake

Miyake-jima is a basaltic stratovolcanic island in the Izu-Bonin arc, Japan, and has erupted quasiperiodically with an approximate interval of 20 years; the recent activities took place in 1940, 1962, and 1983. The eruption in 2000 was expected in this sense; however, what actually happened was totally unexpected: a new caldera was formed for the first time in the past 2500 years (**Figure 24**). This caldera-forming process was recorded with contemporary geophysical equipments.

Figure 25 shows the seismicity observed during the 2000 Miyake-jima activity. The earthquake swarm started right beneath the volcano, and migrated to the southwest ((Uhira *et al.*, 2005), not well-resolved in **Figure 25**), which may correspond to the subsurface migration of magma beneath the volcano. The swarm activity next shifted to northwest of the island, indicating a major subsurface magma migration from the volcano to the outside dike system. After a small summit eruption, the caldera formation took place, and a number of low-frequency earthquakes are observed beneath the summit area. It appears that sucking of magma from the magma storage system beneath the volcano to the northwest dike system, and the resulting magma vacancy in the volcano, are the direct causes of the caldera formation (Furuya *et al.*, 2003).

During roughly 40 days of the caldera formation, a number of peculiar bell-shaped long-period (50 s) seismic (velocity) signals, as well as steps in tiltmeters, are observed once or twice a day (**Figure 26**). Based on

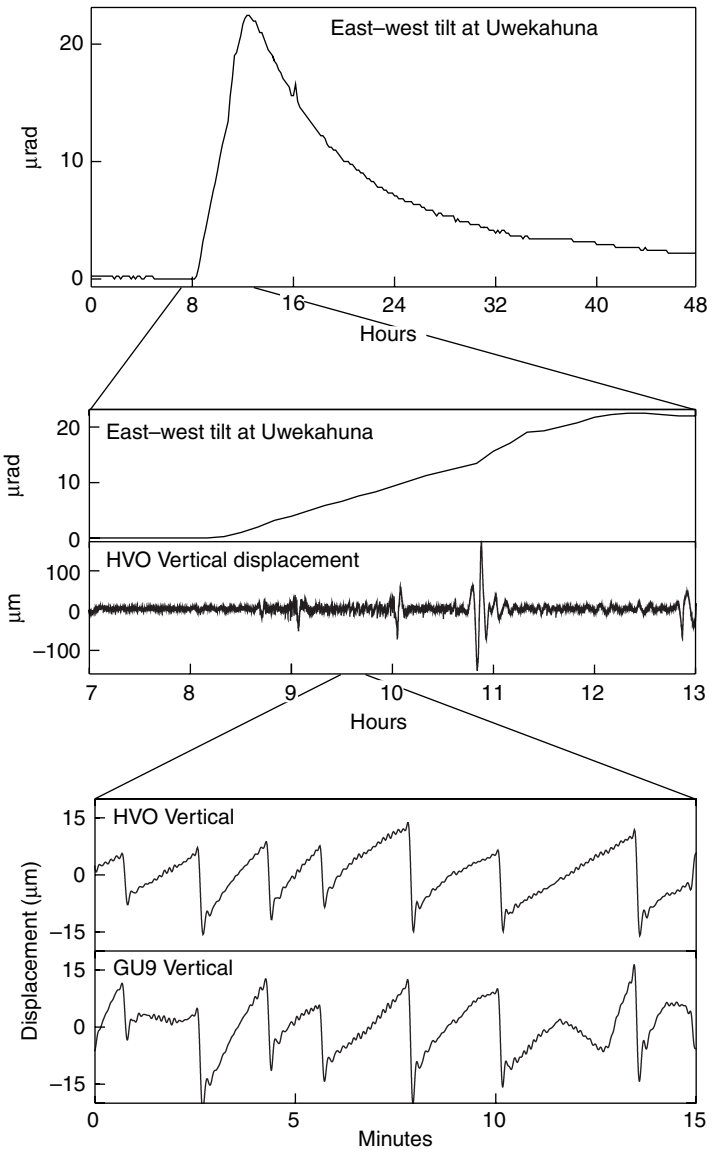

Figure 23 Tilt and broadband record observed around the summit caldera of Kilauea. Adapted from Ohminato T, Chouet B, Dawson P, and Kedar S (1998) Waveform inversion of very long period impulsive signals associated with magmatic injection beneath Kilauea Volcano, Hawaii. *Journal of Geophysical Research* 103: 23839–23862.

the moment tensor inversion of the near-field and far-field broadband seismic records, Kumagai *et al.*, (2001) associated these long-period velocity pulses with inflations of a nearly vertical crack-like magma chamber due to its pressure increase as response to the repetitive stick-slip-type falling of a piston-like mass within the conduit, that results in the caldera formation at the summit. Analyzing the signals of the same sequence of events recorded by the tiltmeters and broadband seismometers deployed in the island, Fujita *et al.* (2004) arrived at a different conclusion. They suggest that these events are caused by a cyclic expansion of a subsurface sill-like magma plumbing system, and introduce a model based on a two-phase flow instability, called a pressure drop oscillation as the mechanism for the repeated activity. Either proposed model seems to explain a part of the observations, but not all. Although the available data may not be able to eventually resolve the difference, nevertheless the 2000 Miyake-jima activity has provided us a rare opportunity to observe a caldera-forming event with contemporary geophysical instruments.

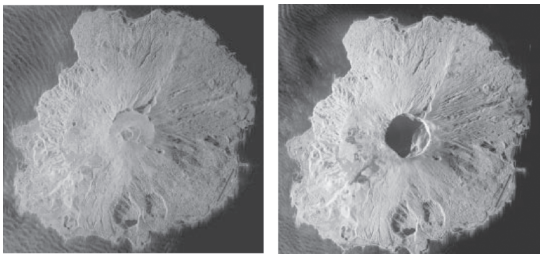

Figure 24 Airborne SAR images of Miyake-jima Volcano before and after the 2000 caldera formation. Adapted from Kumagai H, Ohminato T, and Nakano M, *et al*. (2001) Very-long-period seismic signals and caldera formation at Miyake island, Japan. *Science* 293: 687–690.

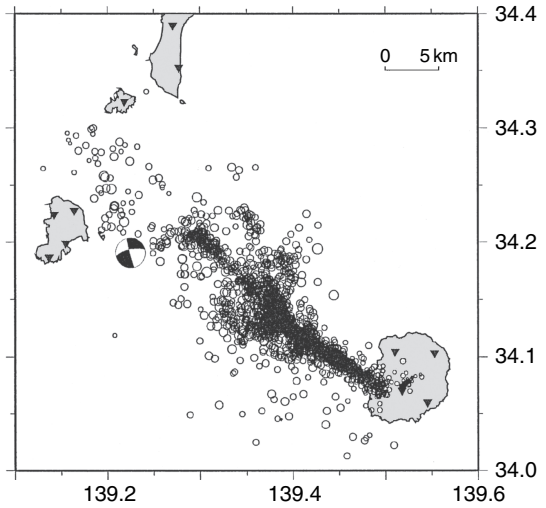

Figure 25 The seismicity of the 2000 Miyake-jima activity. Adapted from Sakai S, Yamada T, and Ide S, *et al*. (2001) Magma migration from the point of view of seismic activity in the volcanism of Miyake-jima island in 2000. *Journal of Geography* 110: 145–155.

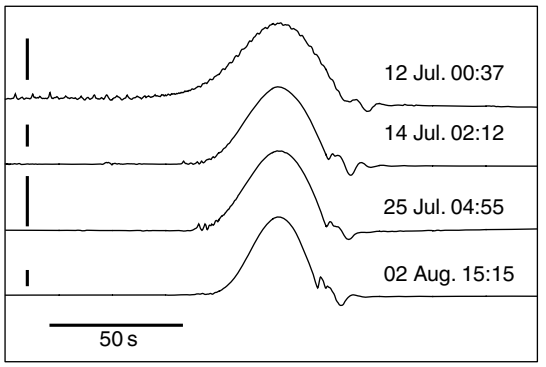

Figure 26 Vertical-component near-field velocity waveforms observed in the Miyake-jima island. Adapted from Kumagai H, Ohminato T, and Nakano M, *et al*. (2001) Very-long-period seismic signals and caldera formation at Miyake island, Japan. *Science* 293: 687–690.

4.13.6.4 Stromboli

Stromboli is one of the Aeolian islands of Italy, and has been almost continuously in eruption for more than at least 2000 years. In contrast to the widely used term 'Strombolian eruption' that is undiscerningly used to describe a variety of volcanic eruptions, the activity of Stromboli is characterized by short-term explosive bursts of lava ejected into the air. Since they eject relatively viscous basaltic lava, building up of the gas pressure is required to fragment the magma, and results in intermittent episodic explosions.

From the seismic point of view, such activities generate a considerable number of explosion quakes, persistent volcanic tremors, and long-period signals. One of the most characteristic features of seismic activities at Stromboli is the extremely wide frequency contents of these signals (**Figure 27**). Spindle-shaped signals superimposed on background continuous tremor are generated by summit eruptions, and the nature of these short-period signals has been extensively studied by many researchers (e.g., Del Pezzo *et al*., 1974; Del Pezzo, 1992; Ripepe and Gordeev, 1999; Saccorotti and Del Pezzo, 2000). These studies shed new light on the seismic activity of the volcano, which is mainly characterized by a very shallow seismicity. Such very shallow origin of the seismic signals is also confirmed by the analyses of seismic array observations (e.g., Chouet *et al*., 1997; Saccorotti and Del Pezzo, 2000), and the sources of explosion quakes and tremors are located at depths shallower than 200 m beneath the summit crater.

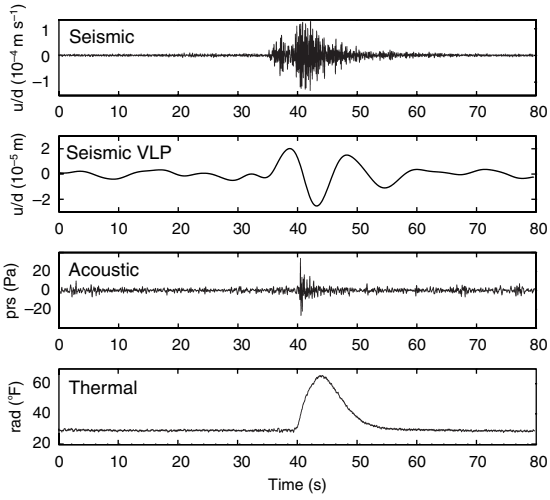

Figure 27 Example of the synchronous occurrence of seismic, acoustic, and thermal signals observed in Stromboli. From Ripepe *et al*., unpublished data.

Recent observations using broadband seismometers reveal the existence of VLP signals with a period of about 10 s which are accompanied with explosions, and give additional constraints on the understanding of Strombolian activities (e.g., Neuberg *et al.*, 1994; Chouet *et al.*, 2003). Analyses of broadband seismograms using the independent component analysis method indicate that further longer-period signals (30–40 s) are generated at almost the same region as the VLP signals (De Martino *et al.*, 2005).

Based on various field observations and laboratory experiments, Ripepe and Gordeev (1999) and Ripepe *et al.* (2001) arrived at a model of Strombolian explosions that is a reminiscent of the analog experimental model by Jaupart and Vergniolle (1989), in which dissolved gas bubbles are trapped at the roof of a magma reservoir as a foam layer and the periodical collapse of the layer causes ascent of gas slugs through a vertical conduit connecting the reservoir and the surface vent. The growth, flow, and burst of the coalescent gas bubbles observed in their laboratory experiments well capture the characteristics of sequential occurrence of very-long-period/short-period seismic signals, acoustic signals, and thermal/light emissions observed at Stromboli. **Figure 28** shows such a direct link between gas flux, magma volume flux, and seismicity, where the balance between gas/magma flux and gas overpressurization appears to determine the type of activities (i.e., effusive or explosive). The common trend in the VLP event rate and the SO_2 emission rate during the effusive phase suggests that the rate of gas flux controls the frequency of foam coalescence and the development of gas slugs which generate VLP signals; the decrease in SO_2 and VLP rates coincides with the increase in the explosion rate at the summit measured by the count of thermal transients and in the amplitude of acoustic pressure; this may be understood in terms of the reduction of gas/magma supplies that results in sealing of eruptive fractures and the upward migration of magma in the conduit.

Performing detailed analyses of the broadband network data, Chouet *et al.* (2003) concluded that the source mechanism of VLP events associated with Strombolian explosions consists of both moment tensor and single force components, which respectively correspond to the opening/closing of an inclined crack just beneath the active vents and the magma flow in the conduit caused by the piston-like rise of a gas slug. To investigate the behavior of coalescence and ascent of gas slugs in such an inclined conduit, James *et al.* (2004) carried out laboratory experiments of the two-phase flow in vertical and inclined pipes, and demonstrated that the inclination of the conduit may play an important role in controlling the flow types and size/velocity distributions of gas slugs in the fluid-filled conduit.

In spite of the difference between models in details, these results suggest that understanding of the bubble dynamics may be essential to elucidate the source process of the seismic signals and the dynamics of Strombolian activities.

4.13.7 Other Volcano-Specific Issues

4.13.7.1 Explosion Quakes

Explosion quakes are observed when explosive eruptions occur (e.g., **Figures 3** and **4**). An explosive volcanic eruption (vulcanian type) can be macroscopically understood as the deflation process of a reservoir system beneath a volcano which may be observed by geodetic (e.g., Ishihara, 1990) or broadband seismic (e.g., **Figure 6**) means. The source mechanism of the accompanied explosion quake may be represented by a combination of a single force and an implosive moment tensor (**Figure 11**). Since the pioneering work of Kanamori *et al.* (1984), there are now a number of observations to quantify the force mechanism and size of volcanic explosions (e.g., Nishimura *et al.*, 1995; Chouet *et al.*, 2005; Ohminato *et al.*, 2006).

Explosion quakes are extensively studied at Sakurajima Volcano, Japan; comparing seismic and video records, Ishihara (1985) demonstrated that explosion quakes occur at a depth of 1–2 km beneath the active crater about a few seconds prior to the explosive eruptions at the summit which generate air shock waves. Uhira and Takeo (1994) showed that an explosive and implosive cylindrical moment tensor component at the source depth is the dominating source mechanism for the explosion quakes. By carefully analyzing borehole seismic network records, Tameguri *et al.* (2002) were able to decompose explosion quakes into two processes: the first one is an isotropic expansion followed by a contraction of a cylinder at a depth of 2 km, and the second is an isotropic expansion and subsequent horizontal contraction at depths of 0.25–0.5 km beneath the crater bottom, which occur about 1 s after the onset of the first and coincide with the generation of the shock wave. The plausibility of this second process was numerically demonstrated by Nishimura and Chouet (2003), who

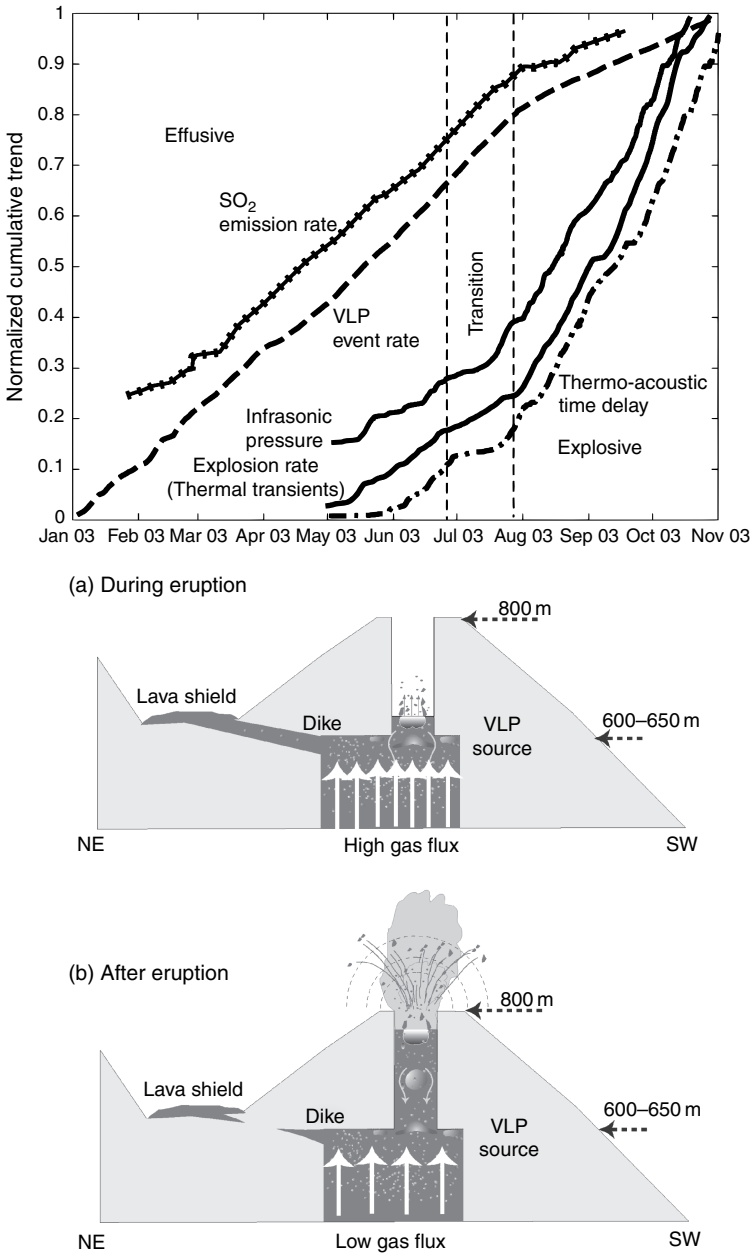

Figure 28 Example of the relation between gas flux rate and seismic/acoustic activities. During the lava effusion phase (model A), few explosions at the summit were observed while the VLP seismicity well correlated with the SO_2 emission rate. On the other hand, in the explosive phase (model B), magma rose up in the conduit due to the sealing of eruptive fractures, resulting in the gas overpressurization and the explosive activity at the summit craters. Adapted from Ripepe M, Marchetti E, and Ulivieri G, *et al*. (2005) Effusive to explosive transition during the 2003 eruption of Stromboli Volcano. *Geology* 33: 341–344.

considered the behavior of a reservoir–conduit system embedded in a homogeneous crust which is filled with a compressive fluid; it was shown that an abrupt pressure increase occurs just beneath the vent which can generate pulse-like Rayleigh waves as observed by Tameguri *et al.* (2002), and that the strength of the lid played an important role in defining eruption types.

Scaling law of volcanic explosions. Nishimura (1998) showed that the far-field displacement due to an explosion is proportional to the area (square of radius) of the crater vent, and obtained a scaling law of volcanic explosion quakes, as similar to that of earthquakes. **Figure 29** compares the vent radii and estimated seismic magnitudes of the largest event for

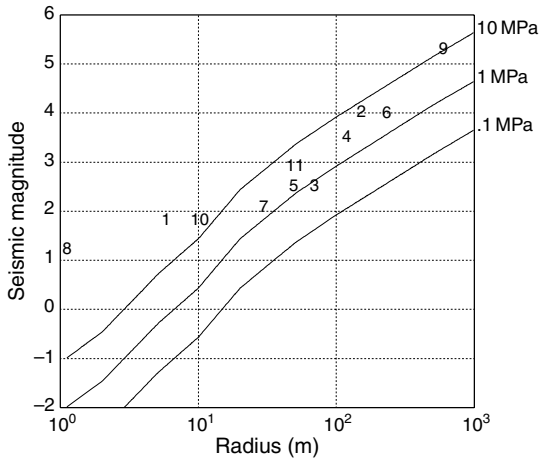

Figure 29 Relation between the seismic magnitude of eruption quakes and the observed vent radius. Numbers from 1 to 11 indicate representative points of different volcanos. Lines show theoretical relation for assumed initial excess pressures. Adapted from Nishimura T (1998) Source mechanisms of volcanic explosion earthquakes: Single force and implosive sources. *Journal of Volcanology and Geothermal Research* 86: 97–106.

studied volcanoes by various investigators; it shows that the magnitude is essentially proportional to the cross-sectional area of the vent for vent radii ranging from 10 to 600 m, as predicted by the theory, and that the initial excess pressure in the reservoir is of the order of a few magapascals, a similar value as the stress drops of earthquakes. This suggests that the size of explosion quakes may be estimated by knowing the vent radius, although it does not necessarily imply that it is possible to predict the size of future eruptions, as it is not guaranteed that the size of present vent is the same for the future ones.

4.13.7.2 Triggered Seismicity

It has been well known among local observers that volcanoes are 'sensitive', as seismicity there often shows changes apparently associated with external disturbances (tides or large earthquakes). For example, Sassa (1936) documented diurnal and semi-diurnal periodicities in the occurrence of volcanic seismicity of Aso Volcano. McNutt and Beavan (1981) also suggested a tidal correlation of seismicity at Pavlof Volcano (cf. Emter, 1997).

There are also convincing lines of evidence that the passage of large amplitude seismic waves dynamically trigger seismicity, especially at volcanoes. Hill *et al.* (1993) documented the seismicity increase in Long Valley caldera, USA, following the $M_w = 7.3$ 1992 Landers earthquake, California (also Gomberg *et al.*, 2001; Prejean *et al.*, 2004). Brodsky and Prejean (2005) made a systematic survey of remotely triggered seismicity at Long Valley; showing the evidence for a frequency-dependent triggering threshold, they concluded that long-period (>30 s) waves are more effective at generating local seismicity than short-period waves of comparable magnitude; among the several proposed mechanisms for such remote dynamic triggering, they suggested that the mechanism that invokes fluid flow through a porous medium can produce such a frequency dependence of triggering threshold (~5 kPa). This mechanism also seems to explain why volcanoes are sensitive to external disturbances, as unclogging fractures to drive fluid flow (Brodsky *et al.*, 2003) may be easily initiated in volcanic/geothermal areas where the constant precipitation from volcanic fluids generate fragile blockages in fractures and faults. West *et al.* (2005) observed periodically (20–30 s) triggered seismicity at Mt. Wrangell, Alaska, when long-period Rayleigh waves generated by the $M_w = 9.0$ 2004 Sumatra earthquake swept across Alaska, and concluded that the extensional stresses of ~25 kPa due to the Rayleigh waves triggered shear failure on normal faults, which may be also influenced by the aforementioned fluid pumping mechanism. These observations suggest that the presence of ample fluid in volcanic systems makes them ideal experimental field for elucidating the earthquake-triggering mechanism.

4.13.8 Concluding Remarks

One of the ultimate goals of volcano seismology is to extract quantitative information about the volcanic fluid transport systems beneath active volcanoes and to utilize such information for forecasting short- and long-term eruptive behaviors. As described in this chapter, macroscopic behaviors of dynamic interactions between volcanic fluids and volcanic edifices have been extensively studied in volcano seismology, and significant progress has been made; the observational/numerical/experimental studies have established firm foundations for explaining the macroscopic processes responsible for generating observed volcanic seismic signals and other related volcanic activities. Considering the rapid progress in technologies for the field observations and numerical simulations, the future of these lines of studies seems to be promising; the accumulation of high-quality digital data at different

volcanoes around the world will further bring significant advances in volcano seismology, as well as volcanology in general; the increase in computer power remarkably extends our capability to simulate complicated dynamic interactions between phases, and enables us to identify and separate distinct signatures of volcanic seismic signals; the recent advance in high-sampling, high-precision GPS and InSAR observations may also help our understanding from the observational aspect.

Nevertheless, our understanding of the elementary physics of multiphase systems, such as the dynamics of bubbles in magmatic fluids and their flows, is still immature, although such understanding fused with the established studies are indispensable for the elucidation of the whole volcanic fluid systems. For instance, recently James *et al.* (2006) experimentally demonstrated that the geometry of the conduit is the key parameter governing the flow pattern of ascending slugs in viscous magma which act as a trigger/source of volcanic seismic signals. Such a parameter of the conduit system may be retrieved by acoustic measurements as demonstrated by Garcés *et al.* (2000), and the integration of these studies will provide a great feedback to volcano seismology. Such studies on the modeling of physical processes, in cooperation with multiparameter observations and numerical simulations, may bring a new boost to volcano seismology in the near future. Volcano seismology, thus, remains to be one of the most challenging fields in Earth science as an integrated science of multidisciplinary researches on multiscale/multiphase systems.

References

Aki K (1957) Space and time spectra of stationary stochastic waves with special reference to microtremors. *Bulletin of the Earthquake Research Institute, University of Tokyo* 35: 415–456.

Aki K (1984) Evidence for magma intrusion during the Mommoth Lakes earthquakes of May 1980 and implications of the absence of volcanic (harmonic) tremor. *Journal of Geophysical Research* 89: 7689–7696.

Aki K, Fehler M, and Das S (1977) Source mechanism of volcanic tremor: Fluid-driven crack models and their application to the 1963 Kilauea eruption. *Journal of Volcanology and Geothermal Research* 2: 259–287.

Aki K and Koyanagi R (1981) Deep volcanic tremor and magma ascent mechanism under Kilauea, Hawaii. *Journal of Geophysical Research* 86: 7095–7109.

Aki K and Lee WHK (2003) Appendix 1 – Glossary of Interest to Earthquake and Engineering Seismologists. In: Lee WHK, Kanamori H, Jennings P, and Kisslinger C (eds.) *International Handbook of Earthquake & Engineering Seismology*, Part B, pp. 1793–1856. New York: Academic Press.

Aki K and Richards PG (2002) *Quantitative Seismology,* 2nd edn. Sausalito, CA: University Science Books.

Alidibirov M and Dingwell DB (1996) Magma fragmentation by rapid decompression. *Nature* 380: 146–149.

Almendros J, Chouet B, and Dawson P (2001) Spatial extent of a hydrothermal system at Kilauea Volcano, Hawaii, determined from array analyses of shallow long-period seismicity. 2: Result. *Journal of Geophysical Research* 106: 13581–13598.

Almendros J, Chouet B, Dawson P, and Bond T (2002a) Identifying elements of the plumbing system beneath Kilauea Volcano, Hawaii, from the source locations of very-long-period signals. *Geophysical Journal International* 148: 303–312.

Almendros J, Chouet B, Dawson P, and Huber C (2002b) Mapping the sources of the seismic wavefield at Kilauea volcano, Hawaii, using data recorded on multiple seismic antennas. *Bulletin of the Seismological Society of America* 92: 2333–2351.

Aoyama H and Takeo M (2001) Wave properties and focal mechanisms of N-type earthquakes at Asama volcano. *Journal of Volcanology and Geothermal Research* 105: 163–182.

Arciniega-Ceballos A, Chouet B, and Dawson P (1999) Very long-period signals associated with vulcanian explosions at Popocatepetl volcano. *Geophysical Research Letters* 26: 3013–3016.

Arciniega-Ceballos A, Chouet B, and Dawson P (2003) Long-period events and tremor at Popocatepetl volcano (1994–2000) and their broadband characteristics. *Bulletin of Volcanology* 65: 124–135.

Aster R, Mah S, Kyle P, *et al.* (2003) Very long period oscillations of Mount Erebus Volcano. *Journal of Geophysical Research* 108: 2522.

Auger E, D'Auria L, Martini M, Chouet B, and Dawson P (2006) Real-time monitoring and massive inversion of source parameters of very long period seismic signals: An application to Stromboli volcano. *Geophysical Research Letters* 33: L04301.

Backus G and Mulcahy M (1976) Moment tensors and other phenomenological descriptions of seismic sources. I: Continuous displacements. *Geophysical Journal of the Royal Astronomical Society* 46: 341–361.

Balmforth EJ, Craster RV, and Rust AC (2005) Instability in flow through elastic conduits and volcanic tremor. *Journal of Fluid Mechanics* 527: 353–377.

Ben-Menahem A and Singh SJ (1981) *Seismic Waves and Sources*. Berlin: Springer.

Benoit JP and McNutt SR (1997) New constraints on source processes of volcanic tremor at Arenal Volcano, Costa Rica, using broadband seismic data. *Geophysical Research Letters* 24: 449–452.

Biot MA (1952) Propagation of elastic waves in a cylindrical bore containing a fluid. *Journal of Applied Physics* 23: 997–1005.

Biot MA (1956) The theory of propagation of elastic waves in a fluid-saturated porous solid. I: Low-frequency range. *Journal of the Acoustical Society of America* 28: 168–178.

Brodsky EE and Prejean SG (2005) New constraints on mechanisms of remotely triggered seismicity at Long Valley Caldera. *Journal of Geophysical Research* 110: B04302.

Brodsky EE, Roeloffs E, Woodcock D, Gall I, and Manga M (2003) A mechanism for sustained groundwater pressure changes induced by distant earthquakes. *Journal of Geophysical Research* 108: 2390.

Brodsky EE, Sturtevant B, and Kanamori H (1998) Earthquakes, volcanoes, and rectified diffusion. *Journal of Geophysical Research* 103: 23827–23838.

Chouet B (1985) Excitation of a buried magmatic pipe: A seismic source model for volcanic tremor. *Journal of Geophysical Research* 90: 1881–1893.

Chouet B (1986) Dynamics of a fluid-driven crack in three dimensions by the finite difference method. *Journal of Geophysical Research* 91: 13967–13992.

Chouet B (1992) A seismic model for the source of long-period events and harmonic tremor. In: *Volcanic Seismology*, pp. 133–156. Berlin: Springer.

Chouet B (1996a) Long-period volcano seismicity: Its source and use in eruption forecasting. *Nature* 380: 309–316.

Chouet B (1996b) New methods and future trends in seismological volcano monitoring. In: *Monitoring and Mitigation of Volcano Hazards*, pp. 23–97. New York: Springer.

Chouet B (2003) Volcano seismology. *Pure and Applied Geophysics* 160: 739–788.

Chouet B, Dawson P, and Arciniega-Ceballos A (2005) Source mechanism of vulcanian degassing at Popocatepetl volcano, Mexico, determined from waveform inversions of very long period signals. *Journal of Geophysical Research* 110: B07301.

Chouet B, Dawson P, Ohminato T, *et al.* (2003) Source mechanisms of explosions at Stromboli Volcano, Italy, determined from moment-tensor inversions of very-long-period data. *Journal of Geophysical Research* 108: 2019.

Chouet B and Julian BR (1985) Dynamics of an expanding fluid-filled crack. *Journal of Geophysical Research* 90: 11187–11198.

Chouet B, Luca GD, Milana G, Dawson PB, Martini M, and Scarpa R (1998) Shallow velocity structure of Stromboli Volcano, Italy, derived from small-aperture array measurements of Strombolian tremor. *Bulletin of the Seismological Society of America* 88: 653–666.

Chouet B, Page RA, Stephens CD, Lahr JC, and Power JA (1994) Precursory swarms of long-period events at Redoubt Volcano (1989–1990), Alaska: Their origin and use as a forecasting tool. *Journal of Volcanology and Geothermal Research* 62: 95–135.

Chouet B, Saccorotti G, Martini M, *et al.* (1997) Source and path effects in the wave fields of tremor and explosions at Stromboli Volcano, Italy. *Journal of Geophysical Research* 102: 15129–15150.

Crosson RS and Bame DA (1985) A spherical source model for low frequency volcanic earthquake. *Journal of Geophysical Research* 90: 10237–10247.

Dahm T (1996) Relative moment tensor inversion based on ray theory: Theory and synthetic tests. *Geophysical Journal International* 124: 245–257.

Dawson P, Dietel C, Chouet B, Honma K, Ohminato T, and Okubo P (1998) A digitally telemetered broadband seismic network at Kilauea Volcano, Hawaii. *US Geological Survey, Open File Report* 98–108: 1–121.

Dawson P, Whilldin D, and Chouet B (2004) Application of near real-time radial semblance to locate the shallow magmatic conduit at Kilauea Volcano, Hawaii. *Geophysical Research Letters* 31: L21606.

De Luca G, Scarpa R, Del Pezzo E, and Simini M (1997) Shallow structure of Mt. Vesuvius volcano, Italy, from seismic array analysis. *Geophysical Research Letters* 24: 481–484.

De Martino S, Falanga M, Scarpa R, and Godano C (2005) Very-long-period volcanic tremor at Stromboli, Italy. *Bulletin of the Seismological Society of America* 95: 1186–1192.

Del Pezzo E (1992) Wave polarization and location of the source of the explosion quakes at Stromboli volcano. In: Gasperini P, Scarpa R, and Aki K (eds.) *Volcanic Seismology*, pp. 279–296. Heidelberg: Springer.

Del Pezzo E, Guerra I, Bascio AL, Luongo G, Nappi G, and Scarpa R (1974) Microtremors ad volcanic explosions at Stromboli - Part 2. *Bulletin of Volcanology* 38: 1023–1036.

Dreger DS, Tkali H, and Johnston M (2000) Dilational processes accompanying earthquakes in the Long Valley Caldera. *Science* 288: 122–125.

Dreier R, Widmer R, Schick R, and Zurn W (1994) Stacking of broad-band seismograms of shocks at Stromboli. *Acta Vulcanologica* 5: 165–172.

Dziewonski AM, Chou TA, and Woodhouse JH (1981) Determination of earthquake source parameters from waveform data for studies of global and regional seismicity. *Journal of Geophysical Research* 86: 2825–2852.

Eissler HK and Kanamori H (1987) A single-force model for the 1975 Kalapana, Hawaii, earthquake. *Journal of Geophysical Research* 92: 4827–4836.

Ekström G, Nettles M, and Abers GA (2003) Glacial earthquakes. *Science* 302: 622–624.

Emter D (1997) Tidal triggering of earthquakes and volcanic events. In: Wilhelm H, Zürn W, and Wenzel HG (eds.) *Tidal Phenomena, Lecture Notes in Earth Sciences*, pp. 293–309. Berlin: Springer.

Eshelby JD (1957) The determination of the elastic field of an ellipsoidal inclusion, and related problems. *Proceedings of the Royal Society of London A* 241: 376–396.

Falsaperla S, Langer H, Martinelli B, and Schick R (1994) Seismic measurements on Stromboli volcano in a wide frequency range. *Acta Vulcanologica* 5: 173–178.

Ferrazzini V and Aki K (1987) Slow waves trapped in a fluid-filled infinite crack: Implication for volcanic tremor. *Journal of Geophysical Research* 92: 9215–9223.

Ferrazzini V, Aki K, and Chouet B (1991) Characteristics of seismic waves composing Hawaiian volcanic tremor and gas-piston events observed by a near-source array. *Journal of Geophysical Research* 96: 6199–6209.

Ferrick M, Qamar A, and Lawrence WFS (1982) Source mechanism of volcanic tremor. *Journal of Geophysical Research* 87: 8675–8683.

Foulger GR, Julian BR, Hill DP, Pitt AM, Malin PE, and Shalev E (2004) Non-double-couple microearthquakes at Long Valley caldera, California, provide evidence for hydraulic fracturing. *Journal of Volcanology and Geothermal Research* 132: 45–71.

Fujita E and Ida Y (2003) Geometrical effects and low-attenuation resonance of volcanic fluid inclusions for the source mechanism of long-period earthquakes. *Journal of Geophysical Research* 108: 2118.

Fujita E, Ida Y, and Oikawa J (1995) Eigen oscillation of a fluid sphere and source mechanism of harmonic volcanic tremor. *Journal of Volcanology and Geothermal Research* 69: 365–378.

Fujita E, Ukawa M, and Yamamoto E (2004) Subsurface cyclic magma sill expansions in the 2000 Miyakejima volcano eruption: Possibility of two-phase flow oscillation. *Journal of Geophysical Research* 109: B04205.

Furuya M, Okubo S, Sun W, *et al.* (2003) Spatiotemporal gravity changes at Miyakejima Volcano, Japan: Caldera collapse, explosive eruptions and magma movement. *Journal of Geophysical Research* 108: 2219.

Garcés M, McNutt SR, Hansen RA, and Eichelberger JC (2000) Application of wave-theoretical seismoacoustic models to the interpretation of explosion and eruption tremor signals radiated by Pavlof volcano, Alaska. *Journal of Geophysical Research* 105: 3039–3058.

Gil Cruz F and Chouet B (1997) Long-period events, the most characteristic seismicity accompanying the emplacement and extrusion of a lava dome in Galeras Volcano, Colombia, in 1991. *Journal of Volcanology and Geothermal Research* 77: 121–158.

Gilbert F (1970) Excitation of the normal-modes of the Earth by earthquake sources. *Geophysical Journal of the Royal Astronomical Society* 23: 119–123.

Goldstein P and Archuleta RJ (1991) Deterministic frequency-wavenumber methods and direct measurements of rupture propagation during earthquakes using a dense array: Theory

and methods. *Journal of Geophysical Research* 96: 6173–6185.
Goldstein P and Chouet B (1994) Array measurements and modeling of sources of shallow volcanic tremor at Kilauea Volcano, Hawaii. *Journal of Geophysical Research* 99: 2637–2652.
Gomberg J, Reasenberg PA, Bodin P, and Harris RA (2001) Earthquake triggering by seismic waves following the Landers and Hector Mine earthquakes. *Nature* 411: 462–466.
Gordeev EI, Saltykov VA, Sinitsin VI, and Chebrov VN (1990) Temporal and spatial characteristics of volcanic tremor wave fields. *Journal of Volcanology and Geothermal Research* 40: 89–101.
Hagerty MT, Schwartz SY, Garcés MA, and Protti M (2000) Analysis of seismic and acoustic observations at Arenal Volcano, Costa Rica, 1995–1997. *Journal of Volcanology and Geothermal Research* 101: 27–65.
Hasegawa A and Yamamoto A (1994) Deep, low-frequency microearthquakes in or around seismic low-velocity zones beneath active volcanoes in northeastern Japan. *Tectonophysics* 233: 233–252.
Hasegawa HS and Kanamori H (1987) Source mechanism of the magnitude 7.2 Grand Banks earthquake of November 1929; double couple or submarine landslide? *Bulletin of the Seismological Society of America* 77: 1984–2004.
Hayashi Y and Morita Y (2003) An image of a magma intrusion process inferred from precise hypocentral migrations of the earthquake swarm east of the Izu Peninsula. *Geophysical Journal International* 153: 159–174.
Hellweg P, Seidl D, Brotopuspito KS, and Brustle W (1994) Team investigates activity at Mt. Semeru, Java, volcano. *EOS, Transactions of AGU* 75: 313–317.
Hidayat D, Chouet B, Voight B, Dawson P, and Ratdomopurbo A (2002) Source mechanism of very-long-period signals accompanying dome growth activity at Merapi volcano, Indonesia. *Geophysical Research Letters* 29: 2118.
Hidayat D, Voight B, Langston C, Ratdomopurbo A, and Ebeling C (2000) Broadband seismic experiment at Merapi Volcano, Java, Indonesia: Very-long-period pulses embedded in multiphase earthquakes. *Journal of Volcanology and Geothermal Research* 100: 215–231.
Hill DP, Dawson P, Johnston MJS, Pitt AM, Biasi G, and Smith K (2002) Very-long-period volcanic earthquakes beneath Mammoth Mountain, California. *Geophysical Research Letters* 29: 1370.
Hill DP and Prejean S (2005) Magmatic unrest beneath Mammoth Mountain, California. *Journal of Volcanology and Geothermal Research* 146: 257–283.
Hill DP, Reasenberg PA, Michael A, *et al.* (1993) Seismicity remotely triggered by the magnitude 7.3 Landers, California, earthquake. *Science* 260: 1617–1623.
Hudson JA, Pearce RG, and Rogers RM (1989) Source type plot for inversion of the moment tensor. *Journal of Geophysical Research* 94: 765–774.
Ibanez JM, Del Pezzo E, Almendros J, *et al.* (2000) Seismovolcanic signals at Deception Island volcano, Antarctica: Wave field analysis and source modeling. *Journal of Geophysical Research* 105: 13905–13932.
Ichihara M and Brodsky EE (2006) A limit on the effect of rectified diffusion in volcanic systems. *Geophysical Research Letters*. 33: L02316.
Ichihara M, Rittel D, and Sturtevant B (2002) Fragmentation of a porous viscoelastic material: Implications to magma fragmentation. *Journal of Geophysical Research* 107: 2229.
Ida Y (1996) Cyclic fluid effusion accompanied by pressure change: Implication for volcanic eruptions and tremor. *Geophysical Research Letters* 23: 1457–1460.
Ishihara K (1985) Dynamical analysis of volcanic explosion. *Journal of Geodynamics* 3: 327–349.
Ishihara K (1990) Pressure sources and induced ground deformation associated with explosive eruptions of an andesitic volcano, Sakurajima volcano, Japan. In: Ryan MP (ed.) *Magma Transport and Storage*, pp. 335–356. New York: Wiley.
Iwamura K and Kaneshima S (2005) Numerical simulation of the steam-water flow instability as a mechanism of long-period ground vibrations at geothermal areas. *Geophysical Journal International* 163: 833–851.
James MR, Lane SJ, Chouet B, and Gilbert JS (2004) Pressure changes associated with the ascent and bursting of gas slugs in liquid-filled vertical and inclined conduits. *Journal of Volcanology and Geothermal Research* 129: 61–82.
James MR, Lane SJ, and Chouet BA (2006) Gas slug ascent through changes in conduit diameter: Laboratory insights into a volcano-seismic source process in low-viscosity magmas. *Journal of Geophysical Research* 111: B05201.
Jaupart C and Vergniolle S (1989) The generation and collapse of a foam layer at the roof of a basaltic magma chamber. *Journal of Fluid Mechanics* 203: 347–380.
Johnson JB and Lees JM (2000) Plugs and chugs–seismic and acoustic observations of degassing explosions at Karymsky, Russia and Sangay, Ecuador. *Journal of Volcanology and Geothermal Research* 101: 67–82.
Jousset P, Neuberg J, and Sturton S (2003) Modelling the time-dependent frequency content of low-frequency volcanic earthquakes. *Journal of Volcanology and Geothermal Research* 128: 201–223.
Julian BR (1983) Evidence for dyke intrusion earthquake mechanisms near Long Valley Caldera, California. *Nature* 303: 323–325.
Julian BR (1994) Volcanic tremor: Nonlinear excitation by fluid flow. *Journal of Geophysical Research* 99: 11859–11878.
Julian BR and Foulger GR (1996) Earthquake mechanisms from linear-programming inversion of seismic-wave amplitude ratios. *Bulletin of the Seismological Society of America* 86: 972–980.
Julian BR, Miller AD, and Foulger GR (1997) Non-double-couple earthquake mechanisms at the Hengill-Grensdalur volcanic complex, southwest Iceland. *Geophysical Research Letters* 24: 743–746.
Julian BR, Miller AD, and Foulger GR (1998) Non-double-couple earthquakes. 1: Theory. *Review of Geophysics* 36: 525–549.
Kamo K, Furuzawa T, and Akamatsu J (1977) Some natures of volcanic micro-tremors at the Sakurajima volcano. *Bulletin of the Volcanological Society of Japan* 22: 41–58.
Kanamori H, Ekström G, Dziewonski A, Barker JS, and Sipkin SA (1993) Seismic radiation by magma injection: An anomalous seismic event near Tori Shima, Japan. *Journal of Geophysical Research* 98: 6511–6522.
Kanamori H and Given JW (1982) Analysis of long-period seismic waves excited by the May 18, 1980, eruption of Mount St. Helens - A terrestrial monopole. *Journal of Geophysical Research* 87: 5422–5432.
Kanamori H, Given JW, and Lay T (1984) Analysis of seismic body waves excited by the Mount St. Helens eruption of May 18, 1980. *Journal of Geophysical Research* 89: 1856–1866.
Kanamori H and Mori J (1992) Harmonic excitation of mantle Rayleigh waves by the 1991 eruption of Mount Pinatubo Philippines. *Geophysical Research Letters* 19: 721–724.
Kaneshima S, Kawakatsu H, Matsubayashi H, *et al.* (1996) Mechanism of phreatic eruptions at Aso Volcano Inferred from near-field broadband seismic observations. *Science* 273: 643–645.
Kawakatsu H (1989) Centroid single force inversion of seismic waves generated by landslides. *Journal of Geophysical Research* 94: 12363–12374.

Kawakatsu H (1998) On the realtime monitoring of the long-period seismic wavefield. *Bulletin of the Earthquake Research Institute, University of Tokyo* 73: 267–274 (also in Methods and applications of signal processing in seismic network operations (2002), Springer, pp.251–257).

Kawakatsu H, Kaneshima S, Matsubayashi H, *et al.* (2000) Aso94: Aso seismic observation with broadband instruments. *Journal of Volcanology and Geothermal Research* 101: 129–154.

Kawakatsu H, Ohminato T, and Ito H (1994) 10s-period volcanic tremors observed over a wide area in southwestern Japan. *Geophysical Research Letters* 21: 1963–1966.

Kawakatsu H, Ohminato T, Ito H, *et al.* (1992) Broadband seismic observation at the Sakurajima volcano, Japan. *Geophysical Research Letters* 19: 1959–1962.

Kieffer SW (1977) Sound speed in liquid-gas mixtures: Water–air and water–steam. *Journal of Geophysical Research* 82: 2895–2904.

Kikuchi M and Kanamori H (1982) Inversion of complex body waves. *Bulletin of the Seismological Society of America* 72: 491–506.

Klein FW and Koyanagi RY (1989) The seismicity and tectonics of Hawaii. In: *The Geology of North America*, Vol. N, The Eastern Pacific Ocean and Hawaii, pp. 238–252. Geological Society of America.

Knopoff L and Randall M (1970) The compensated linear-vector dipole: A possible mechanism for deep earthquakes. *Journal of Geophysical Research* 75: 4957–4963.

Kubotera A (1974) Volcanic tremors at Aso volcano. In: Civetta L, Gasparini, Luongo G, and Rapolla A (eds.) *Physical Volcanology*, pp. 29–47. Amsterdam: Elsevier.

Kumagai H (2006) Temporal evolution of a magmatic dike system inferred from the complex frequencies of very long period seismic signals. *Journal of Geophysical Research* 111: B06201.

Kumagai H and Chouet B (1999) The complex frequencies of long-period seismic events as probes of fluid composition beneath volcanoes. *Geophysical Journal International* 138: F7–F12.

Kumagai H and Chouet B (2000) Acoustic properties of a crack containing magmatic or hydrothermal fluids. *Journal of Geophysical Research* 105: 25493–25512.

Kumagai H, Chouet B, and Dawson PB (2005) Source process of a long-period event at Kilauea volcano, Hawaii. *Geophysical Journal International* 161: 243–254.

Kumagai H, Chouet B, and Nakano M (2002) Temporal evolution of a hydrothermal system in Kusatsu-Shirane Volcano, Japan, inferred from the complex frequencies of long-period events. *Journal of Geophysical Research* 107: ESE 9–1.

Kumagai H, Ohminato T, and Nakano M, *et al.* (2001) Very-long-period seismic signals and caldera formation at Miyake island, Japan. *Science* 293: 687–690.

Leet RC (1988) Saturated and subcooled hydrothermal boiling in groundwater flow channels as a source of harmonic tremor. *Journal of Geophysical Research* 93: 4835–4849.

Legrand D, Kaneshima S, and Kawakatsu H (2000) Moment tensor analysis of near-field broadband waveforms observed at Aso Volcano, Japan. *Journal of Volcanology and Geothermal Research* 101: 155–169.

McNutt SR (1996) Seismic monitoring and eruption forecasting of volcanoes: A review of the state-of-the-art and case histories. In: Scarpa R and Tilling RI (eds.) *Monitoring and Mitigation of Volcano Hazards*, pp. 99–146. New York: Springer.

McNutt SR (2002) Volcano seismology. In: Lee WHK, Kanamori H, Jennings P, Kisslinger C (eds.) *International Handbook of Earthquake and Engineering Seismology*, Part A, Ch. 25, pp. 383–406. New York: Academic Press.

McNutt SR (2005) Volcanic seismology. *Annual Review of Earth and Planetary Sciences* 33: 461–491.

McNutt SR and Beavan RJ (1981) Volcanic earthquakes at Pavlof Volcano correlated with the solid earth tide. *Nature* 294: 615–518.

Metaxian J-P and Lasage P (1997) Permanent tremor of Masaya Volcano, Nicaragua: Wave field analysis and source location. *Journal of Geophysical Research* 102: 22529–22545.

Miller AD, Foulger GR, and Julian BR (1998) Non-double-couple earthquakes. 2: Observations. *Review of Geophysics* 36: 551–568.

Minakami T (1974) Seismology of volcanoes in Japan. In: Civetta L, Gasparini P, Luongo G, and Rapolla A (eds.) *Physical Volcanology*, pp. 1–27. Amsterdam: Elsevier.

Mogi K (1958) Relation between the eruptions of various volcanoes and the deformations of the ground surfaces around them. *Bulletin of the Earthquake Research Institute* 36: 99–134.

Molina I, Kumagai H, and Yepes H (2004) Resonances of a volcanic conduit triggered by repetitive injections of an ash-laden gas. *Geophysical Research Letters* 31: L03603.

Mori J, Patia H, McKee C, *et al.* (1989) Seismicity associated with eruptive activity at Langila volcano, Papua New Guinea. *Journal of Volcanology and Geothermal Research* 38: 243–255.

Morrissey MM and Chouet B (1997) Burst conditions of explosive volcanic eruptions recorded on microbarographs. *Science* 275: 1290–1293.

Morrissey MM and Chouet B (2001) Trends in long-period seismicity related to magmatic fluid compositions. *Journal of Volcanology and Geothermal Research* 108: 265–281.

Nakamichi H, Hamaguchi H, Tanaka S, Ueki S, Nishimura T, and Hasegawa A (2003) Source mechanisms of deep and intermediate-depth low-frequency earthquakes beneath Iwate volcano, northeastern Japan. *Geophysical Journal International* 154: 811–828.

Nakano M, Kumagai H, and Chouet B (2003) Source mechanism of long-period events at Kusatsu-Shirane Volcano, Japan, inferred from waveform inversion of the effective excitation functions. *Journal of Volcanology and Geothermal Research* 122: 149–164.

Nakano M, Kumagai H, Kumazawa M, Yamaoka K, and Chouet B (1998) The excitation and characteristic frequency of the long-period volcanic event: An approach based on an inhomogeneous autoregressive model of a linear dynamic system. *Journal of Geophysical Research* 103: 10031–10046.

Nettles M and Ekström G (1998) Faulting mechanism of anomalous earthquakes near Bardarbunga volcano, Iceland. *Journal of Geophysical Research* 103: 17973–17984.

Neuberg J, Luckett R, Baptie B, and Olsen K (2000) Models of tremor and low-frequency earthquake swarms on Montserrat. *Journal of Volcanology and Geothermal Research* 101: 83–104.

Neuberg J, Luckett R, Ripepe M, and Braun T (1994) Highlights from a seismic broad-band array on Stromboli volcano. *Geophysical Research Letters* 21: 749–752.

Nishida K, Kobayashi N, and Fukao Y (2000) Resonant oscillations between the solid earth and the atmosphere. *Science* 287: 2244–2246.

Nishimura T (1998) Source mechanisms of volcanic explosion earthquakes: Single force and implosive sources. *Journal of Volcanology and Geothermal Research* 86: 97–106.

Nishimura T and Chouet B (2003) A numerical simulation of magma motion, crustal deformation, and seismic radiation associated with volcanic eruptions. *Geophysical Journal International* 153: 699–718.

Nishimura T, Hamaguchi H, and Ueki S (1995) Source mechanisms of volcanic tremor and low-frequency earthquakes associated with the 1988–89 eruptive activity of Mt. Tokachi, Hokkaido, Japan. *Geophysical Journal International* 121: 444–458.

Nishimura T, Nakamichi H, Tanaka S, *et al.* (2000) Source process of very long period seismic events associated with the 1998 activity of Iwate Volcano, northeastern Japan. *Journal of Geophysical Research* 105: 19135–19147.

Nishimura T, Ueki S, Yamawaki T, *et al.* (2003) Broadband seismic signals associated with the 2000 volcanic unrest of Mount Bandai, northeastern Japan. *Journal of Volcanology and Geothermal Research* 119: 51–59.

Ohminato T (2006) Characteristics and source modeling of broadband seismic signals associated with the hydrothermal system at Satsuma-iwojima volcano, Japan. *Journal of Volcanology and Geothermal Research* 158: 467–490.

Ohminato T and Chouet B (1997) A free-surface boundary condition for including 3D topography in the finite-difference method. *Bulletin of the Seismological Society of America* 87: 494–515.

Ohminato T, Chouet B, Dawson P, and Kedar S (1998) Waveform inversion of very long period impulsive signals associated with magmatic injection beneath Kilauea Volcano, Hawaii. *Journal of Geophysical Research* 103: 23839–23862.

Ohminato T and Ereditato D (1997) Broadband seismic observations at Satsuma-Iwojima volcano, Japan. *Geophysical Research Letters* 24: 2845–2848.

Ohminato T, Takeo M, Kumagai H, *et al.* (2006) Vulcanian eruptions with dominant single force components observed during the Asama 2004 volcanic activity in Japan. *Earth Planets Space* 58: 583–593.

Pitt AM and Hill DP (1994) Long-period earthquakes in the Long Valley caldera region, eastern California. *Geophysical Research Letters* 21: 1679–1682.

Prejean SG, Hill DP, Brodsky EE, *et al.* (2004) Remotely triggered seismicity on the United States west coast following the Mw 7.9 Denali fault earthquake. *Bulletin of the Seismological Society of America* 94: S348–S359.

Ripepe M, Ciliberto S, and Schiava MD (2001) Time constraints for modeling source dynamics of volcanic explosions at Stromboli. *Journal of Geophysical Research* 106: 8713–8727.

Ripepe M and Gordeev E (1999) Gas bubble dynamics model for shallow volcanic tremor at Stromboli. *Journal of Geophysical Research* 104: 10639–10654.

Ripepe M, Marchetti E, Ulivieri G, *et al.* (2005) Effusive to explosive transition during the 2003 eruption of Stromboli Volcano. *Geology* 33: 341–344.

Ripepe M, Poggi P, Braun T, and Gordeev E (1996) Infrasonic waves and volcanic tremor at Stromboli. *Geophysical Research Letters* 23: 181–184.

Ross A, Foulger GR, and Julian BR (1996) Non-double-couple earthquake mechanisms at The Geysers geothermal area, California. *Geophysical Research Letters* 23: 877–880.

Rowe CA, Aster RC, Kyle PR, Dibble RR, and Schlue JW (2000) Seismic and acoustic observations at Mount Erebus Volcano, Ross Island, Antarctica, 1994–1998. *Journal of Volcanology and Geothermal Research* 101: 105–128.

Rowe CA, Aster RC, Kyle PR, Schlue JW, and Dibble RR (1998) Broadband recording of Strombolian explosions and associated very-long-period seismic signals on Mount Erebus volcano, Ross Island, Antarctica. *Geophysical Research Letters* 25: 2297–2300.

Saccorotti G, Almendros J, Carmona E, Ibanez JM, and Del Pezzo E (2001a) Slowness Anomalies from Two Dense Seismic Arrays at Deception Island Volcano, Antarctica. *Bulletin of the Seismological Society of America* 91: 561–571.

Saccorotti G, Chouet B, and Dawson P (2001b) Wavefield properties of a shallow long-period event and tremor at Kilauea Volcano, Hawaii. *Journal of Volcanology and Geothermal Research* 109: 163–189.

Saccorotti G and Del Pezzo E (2000) A probabilistic approach to the inversion of data from a seismic array and its application to volcanic signals. *Geophysical Journal International* 143: 249–261.

Sakai S, Yamada T, Ide S, *et al.* (2001) Magma migration from the point of view of seismic activity in the volcanism of Miyake-jima island in 2000. *Journal of Geography* 110: 145–155.

Sassa K (1935) Volcanic micro-tremors and eruption-earthquakes (Part 1 of the geophysical studies on the volcano Aso). *Memories of the College of Science, Kyoto Imperial University* 18: 255–293.

Sassa K (1936) Micro-seismometric study on eruption of the Volcano Aso. *Memories of the College of Science, Kyoto Imperial University* 19: 11–56.

Scarpa R and Tilling RI (1996) *Monitoring and Mitigation of Volcanic Hazards*. New York: Springer.

Schmidt RO (1986) Multiple emitter location and signal parameter estimation. *IEEE Transactions on Antennas and Propagation* 34: 276–280.

Schoenberg M and Sen PN (1983) Properties of a periodically stratified acoustic half-space and its relation to a Biot fluid. *Journal of the Acoustical Society of America* 73: 61–67.

Seidl D, Schick R, and Riuscetti M (1981) Volcanic tremors at Etna: A model for hydraulic origin. *Bulletin of Volcanology* 141: 43–56.

Sudo Y and Kong LSL (2001) Three-dimensional seismic velocity structure beneath Aso Volcano, Kyushu, Japan. *Bulletin of Volcanology* 63: 326–344.

Sutton AJ, Elias T, Gerlach TM, and Stokes JB (2001) Implications for eruptive processes as indicated by sulfur dioxide emissions from Kilauea Volcano, Hawaii, 1979–1997. *Journal of Volcanology and Geothermal Research* 108: 283–302.

Takagi N, Kaneshima S, Kawakatsu H, *et al.* (2006) Apparent migration of tremor source synchronized with the change in the tremor amplitude observed at Aso volcano, Japan. *Journal of Volcanology and Geothermal Research* 154: 181–200.

Takei Y and Kumazawa M (1994) Why have the single force and torque been excluded from seismic source models? *Geophysical Journal International* 118: 20–30.

Takeo M (1992) The rupture process of the 1989 offshore Ito earthquakes preceding a submarine volcanic eruption. *Journal of Geophysical Research* 97: 6613–6627.

Takeo M, Hamada N, Kashiwabara S, and Uhira K (1984) Analysis of long-period seismic waves excited by the explosive eruption of Mt. Asama on April 8. *Bulletin of the Volcanological Society of Japan* 29: 31–44.

Takeo M, Yamasato H, Furuya I, and Seino M (1990) Analysis of long-period seismic waves excited by the November 1987 eruption of Izu-Oshima volcano. *Journal of Geophysical Research* 95: 19377–19393.

Tameguri T, Iguchi M, and Ishihara K (2002) Mechanism of explosive eruptions from moment tensor analyses of explosion earthquakes at Sakurajima volcano, Japan. *Bulletin of the Volcanological Society of Japan* 47: 197–216.

Tsutsui T and Sudo Y (2004) Seismic reflectors beneath the central cones of Aso Volcano, Kyushu, Japan. *Journal of Volcanology and Geothermal Research* 131: 33–58.

Uhira K, Baba T, Mori H, Katayama H, and Hamada N (2005) Earthquake swarms preceding the 2000 eruption of Miyakejima volcano, Japan. *Bulletin of Volcanology* 67: 219–230.

Uhira K, Ikeda S, and Takeo M (1994a) Source process of explosion earthquakes deduced from short-period records at Sakurajima volcano. *Bulletin of the Volcanological Society of Japan* 40: 295–310.

Uhira K and Takeo M (1994) The source of explosive eruptions of Sakurajima volcano, japan. *Journal of Geophysical Research* 99: 17775–17789.

Uhira K, Yamasato H, and Takeo M (1994b) Source mechanism of seismic waves excited by proclastic flows observed at Unzen volcano, Japan. *Journal of Geophysical Research* 99: 17757–17773.

Ukawa M and Ohtake M (1987) A monochromatic earthquake suggesting deep-seated magmatic activity beneath the Izu-Ooshima Volcano, Japan. *Journal of Geophysical Research* 92: 12649–12663.

Vergniolle S, Brandeis G, and Mareschal J-C (1996) Strombolian explosions. 2: Eruption dymanics determined form acoustic measurements. *Journal of Geophysical Research* 101: 20449.

Waite GP, Chouet B, Dawson P, and Moran SC (2005) Very-long-period seismic source at Mount St. Helens. *EOS, Transactions of AGU* 86 (Fall Meet. Suppl.,): Abstract V53D–1601.

Wallace TC (1985) A reexamination of the moment tensor solutions of the 1980 Mammoth Lakes earthquakes. *Journal of Geophysical Research* 90: 11171–11176.

Watada S (1995) *Part I: Near-source Acoustic Coupling Between the Atmosphere and the Soild Earth During Volcanic Eruptions*. PhD Thesis, California Institute of Technology.

West M, Sanchez JJ, and McNutt SR (2005) Periodically triggered seismicity at Mount Wrangell, Alaska, after the Sumatra earthquake. *Science* 308: 1144–1146.

White R (1996) Precursory deep long-period earthquakes at Mount Pinatubo: Spatiotemporal link to a basalt trigger. In: Newhall CG and Punongbayan RS (eds.) *Fire and Mud: Eruptions and Lahars of Mount Pinatubo, Philippines*, pp. 307–327. Seattle: University of Washington Press.

Widmer R and Zürn W (1992) Bichromatic excitation of long-period Rayleigh and air waves by the Mount Pinatubo and E1 Chichon volcanic eruptions. *Geophysical Research Letters* 19: 765–768.

Wilson L and Head JW (1981) Ascent and eruption of basaltic magma on the earth and moon. *Journal of Geophysical Research* 86: 2971–3001.

Yamamoto M (2005) *Volcanic Fluid System Inferred from Broadband Seismic Signals*. PhD Thesis, University of Tokyo.

Yamamoto M, Kawakatsu H, Kaneshima S, *et al.* (1999) Detection of a crack-like conduit beneath the active crater at Aso volcano, Japan. *Geophysical Research Letters* 26: 3677–3680.

Yamamoto M, Kawakatsu H, Yomogida K, and Koyama J (2002) Long-period (12 sec) volcanic tremor observed at Usu 2000 eruption: Seismological detection of a deep magma plumbing system. *Geophysical Research Letters* 29: 1329.

Yamamura K (1997) *Slow Waves in Solid-Liquid Two Phase System* (in Japanese). Master's Thesis, University of Tokyo.

Yamamura K and Kwakatsu H (1998) Normal-mode solutions for radiation boundary conditions with an impedance contrast. *Geophysical Journal International* 134: 849–855.

Yamasato H, Fukui K, Uhira K, Hashimoto T, and Hori H (1993) Analysis of seismic and acoustic signals excited by pyroclastic flows at Unzen volcano. *Bulletin of the Volcanological Society of Japan* 38: 79–90.

Relevant Website

http://wwweic.eri.u-tokyo.ac.jp – Grid-Based Real-Time Determination of Moment Tensors (GRiD MT), Earthquake Information Center.